

This document is the accepted manuscript version of the following article:

**Authors:** F. Bosia, V. F. Dal Poggetto, A. S. Gliozzi, G. Greco, M. Lott, M. Miniaci, F. Ongaro, M. Onorato, S. F. Seyyedizadeh, M. Tortello, N. M. Pugno

**Title:** Optimized structures for vibration attenuation and sound control in nature: A review

**Journal:** Matter

**Publisher doi:** 10.1016/j.matt.2022.07.023

This manuscript version is made available under the CC-BY-NC-ND 4.0 license

Originally uploaded to URL:

[http://www.ing.unitn.it/~pugno/NP\\_PDF/PostPrint/2022-MATT-Optimized\\_structures.pdf](http://www.ing.unitn.it/~pugno/NP_PDF/PostPrint/2022-MATT-Optimized_structures.pdf) on 22/10/2022

# Optimized structures for vibration attenuation and sound control in nature: A review

Federico Bosia,<sup>1</sup> Vinicius F. Dal Poggetto,<sup>2</sup> Antonio S. Gliozzi,<sup>1</sup> Gabriele Greco,<sup>2</sup> Martin Lott,<sup>1</sup> Marco Miniaci,<sup>3</sup> Federica Ongaro,<sup>2</sup> Miguel Onorato,<sup>4,6</sup> Seyede F. Seyyedizadeh,<sup>1</sup> Mauro Tortello,<sup>1</sup> and Nicola M. Pugno<sup>2,5,\*</sup>

<sup>1</sup> Department of Applied Science and Technology, Politecnico di Torino, 10129 Torino, Italy

<sup>2</sup> Laboratory for Bioinspired, Bionic, Nano, Meta Materials and Mechanics, Department of Civil, Environmental and Mechanical Engineering, University of Trento, 38123 Trento, Italy

<sup>3</sup> CNRS, Université de Lille, Ecole Centrale, ISEN, Université de Valenciennes, IEMN - UMR 8520, 59000 Lille, France

<sup>4</sup> Department of Physics, University of Torino, 10125 Torino, Italy

<sup>5</sup> School of Engineering and Materials Science, Queen Mary University of London, London E1 4NS, UK

<sup>6</sup> Istituto Nazionale di Fisica Nucleare (INFN), Sezione di Torino, 10125 Torino, Italy

\*Correspondence: nicola.pugno@unitn.it <https://doi.org/10.1016/j.matt.2022.07.023>

## SUMMARY

Nature has engineered complex designs to achieve advanced properties and functionalities through millions of years of evolution. Many organisms have adapted to their living environments by producing extremely efficient materials and structures exhibiting optimized mechanical, thermal, and optical properties, which current technology is often unable to reproduce. These properties are often achieved using hierarchical structures spanning macro-, meso-, micro-, and nanoscales, widely observed in many natural materials like wood, bone, spider silk, and sponges. Thus far, bioinspired approaches have been successful in identifying optimized structures in terms of quasistatic mechanical properties, such as strength, toughness, and adhesion, but comparatively little work has been done as far as dynamic ones are concerned (e.g., vibration damping, noise insulation, sound amplification). In particular, relatively limited knowledge currently exists on how hierarchical structure can play a role in the optimization of natural structures, although concurrent length scales no doubt allow multiple frequency ranges to be addressed. Here, we review the main work that has been done to analyze structural optimization for dynamic mechanical properties, highlighting some common traits and strategies in different biological systems. We also discuss the relevance to bioinspired materials, in particular in the field of phononic crystals and metamaterials, and the potential of exploiting natural designs for technological applications.

**PROGRESS AND POTENTIAL** Several natural architectural designs can be found that have been optimized by nature through evolution in terms of quasi-static mechanical properties. Notable cases can also be found in the field of impact damping and elastic wave manipulation for defense, anti-predatory strategies, sensing, sound and vibration control, focusing, and amplification. We discuss some of the main examples in this review. Hierarchy is shown to be an effective and recurrent element in such design strategies at multiple length scales and, therefore, frequency scales. The observation and study of these optimized systems has the potential to improve the design of artificial, bio-inspired materials with an expected impact in the field of phononic crystals and acoustic metamaterials.

## INTRODUCTION

It is well known that engineering materials such as metals or fiber-reinforced plastics are characterized by high stiffness at the expense of toughness. In particular, these materials do not efficiently dissipate energy via vibration damping. On the other hand, particularly compliant materials, such as rubbers and soft polymers, perform well as dampers, but are lacking in stiffness.<sup>1,2</sup> In this context, biological natural materials such as wood, bone, and seashells, to cite a few cases, represent excellent examples of composite materials possessing both high stiffness and high damping, and thus combine properties that are generally mutually exclusive. This exceptional behavior derives from an evolutionary

optimization process that has taken place over millions of years, driven toward specific functionalities, where the natural rule of survival of the fittest has led to the continuous improvement of biological structure and organization. For instance, spider silk, bone, enamel, and limpet teeth are examples of materials that combine high specific strength and stiffness with outstanding toughness and flaw resistance.<sup>3-8</sup> In these examples, a hierarchical architecture has often been proved to be the responsible for many energy dissipation and crack deflection mechanisms over various size scales, simultaneously contributing to exceptional toughness.<sup>2</sup> Given these numerous examples and the related interesting properties, the rich research field of biomimetics has emerged, with the aim of drawing inspiration from natural structures and implementing them in artificial systems, to bring progress to many technological domains.

Despite rapid progress in the field, studies in biomechanics and biomimetics linking material structure to function have mainly been limited to the quasistatic regime, while the dynamic properties of these materials have been somewhat less investigated, although notable examples of impact tolerance (e.g., the bombardier beetle's explosion chamber<sup>9</sup>) or vibration damping (e.g., the woodpecker skull<sup>10</sup>) have been studied. In fact, the first attempt to analyze biological vibration isolation mechanisms in the woodpecker dates as far back as 1959, when Sielmann<sup>11</sup> found, through dissection and observation, that the cartilage in sutures in its skull have the effect of buffering and absorbing vibration.<sup>11</sup> Furthermore, recent studies have shown that structural hierarchy, which is typical of biological materials, can enhance the performance of artificial metamaterials.<sup>12,13</sup>

As confirmed by these examples, it is reasonable to assume that biological structures whose main function is vibration and impact damping, sound filtering and focusing, transmission of vibrations, and so forth have also been optimized through evolution and that it is possible to look for inspiration in nature for technological applications based on these properties. Starting from this assumption, a growing interest in the superior vibration attenuation properties of biological systems has emerged, and nowadays, applications such as bioinspired dampers are beginning to be used in the protection of precision equipment and the improvement of product comfort.<sup>14</sup> Motivated by this emerging field of research, we provide here a review of some of the main biological systems of interest for their dynamic properties, focusing on the role of structural architecture for the achievement of superior performance.

## IMPACT-RESISTANT STRUCTURES

### Mantis shrimp

Probably the most well-known example of impact-resistant structure in nature is the stomatopod dactyl club. The mantis shrimp (*Odontodactylus scyllarus*) is a crustacean with a hammer-like club that can smash prey (mainly shells) with very high-velocity impacts,<sup>15-17</sup> reaching accelerations of up to 10,000 g, and even generating cavitation in the water.<sup>18</sup> To sustain repeated impacts without failing, the claw requires extreme stiffness, toughness, and impact damping, and has emerged as one of the main biological systems that epitomizes biological optimization for impact damage tolerance.<sup>19</sup>

The exceptional impact tolerance is obtained thanks to the graded multiphase composition and structural organization of three different regions in the claw (Figure 1). The impact region, or striking surface, is dominated by oriented mineral crystals (hydroxyapatite),

---

arranged so that they form pillars perpendicular to the striking surface. A second region, called the periodic region, backs up the impact zone and is mainly constituted by chitosan. This area, which lies just beneath the impact zone, is stacked at different (helicoidal) orientations, generating crack stopping and deviation. Thus, the structure consists of a multiphase composite of oriented stiff (crystalline hydroxyapatite) and soft (amorphous calcium phosphate and carbonate) components, with a highly expanded helicoidal organization of the fibrillar chitinous

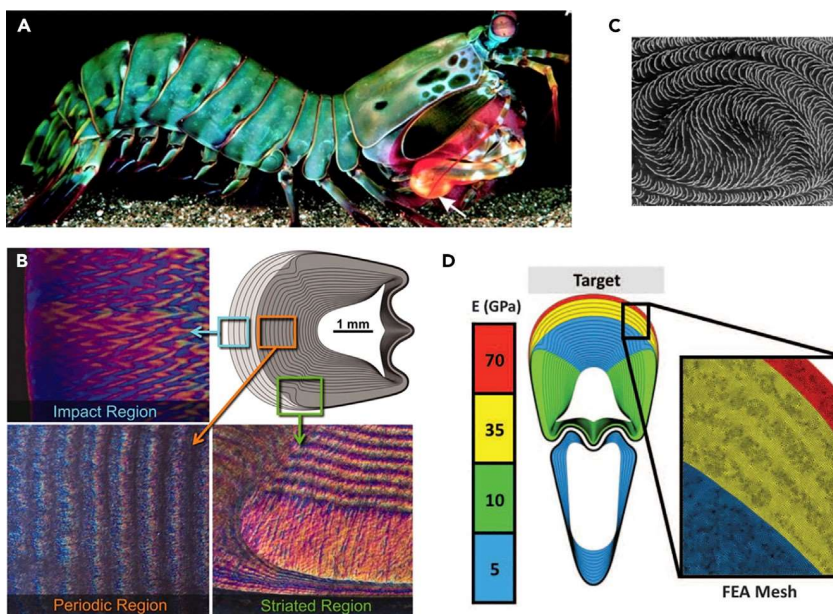


Figure 1. Impact damping in mantis shrimp dactyl clubs

- (A) Peacock mantis shrimp, with highlighted raptorial dactyl clubs to strike hard objects (adapted from Patek and Caldwell<sup>18</sup>).
- (B) Morphological features of the clubs, in cross-section view, divided into an impact region, aperiodic region, and a striated region.
- (C) Scanning electron micrograph of the coronal cross section, showing reinforcing fiber helicoidal arrangement.
- (D) Schematic of a finite-element model accounting for graded material properties (adapted from Weaver et al.<sup>19</sup>). organic matrix, leading to effective damping of high-energy loading events.<sup>19,20</sup> The impact surface region of the dactyl club also exhibits a quasi-plastic contact response due to interfacial sliding and rotation of fluorapatite nanorods, leading to localized yielding and enhanced energy damping.<sup>21</sup>

Interestingly, it has been found that the mantis shrimp also displays another highly efficient impact-damping structure, since it has evolved a specialized shield in its tail segment called telson, which absorbs the blows from other shrimps during ritualized fighting.<sup>22</sup> The telson is a multiscale structure with a concave macromorphology, ridges on the outside, and a well-defined pitch-graded helicoidal fibrous microarchitecture on the inside, which also provides optimized damage tolerance.<sup>23,24</sup>

#### Woodpecker skull

Another well-known example of a highly impact-resistant system in nature is that of the woodpecker skull and beak, which repeatedly strike wooden surfaces in trees at a frequency of about 20 Hz, a speed of up to 7 m/s, and accelerations of the order of 1,200 g, while avoiding brain injury.<sup>10,25</sup> This structure has been widely studied to draw inspiration for impact-attenuation and shock-absorbing applications and biomimetic

isolation.<sup>14</sup> Limiting our observations to the head, and neglecting the body, feathers, and feet (which could also play a role), the woodpecker emerges as a very complex and rich system, from the mechanical and structural point of view, at different spatial scales: macro-, micro-, and nanoscale. The head is mainly formed by the beak, hyoid bone, skull, muscles, ligaments, and brain.<sup>26</sup>

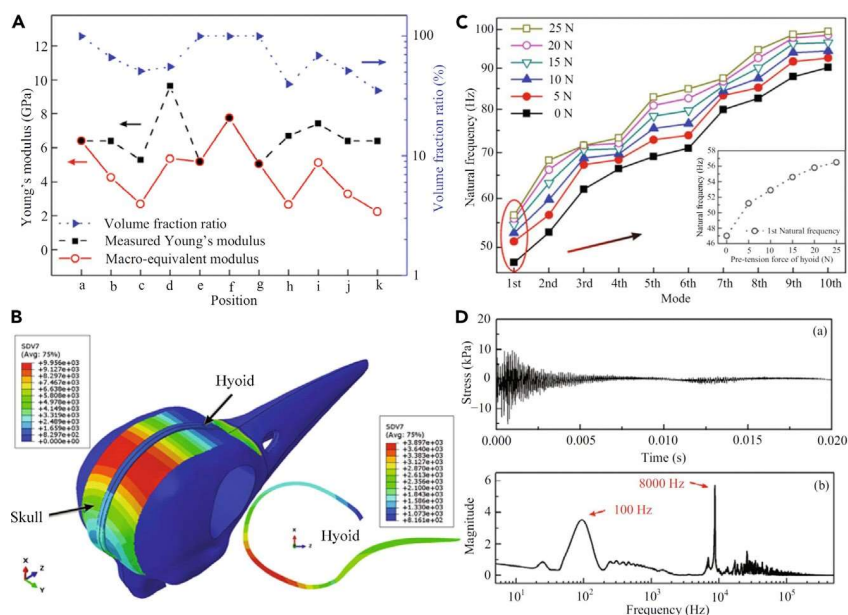


Figure 2. Vibration attenuation in the woodpecker skull (adapted from Zhu et al.<sup>31</sup>) (A) Volume fraction ratio of skull bone, local measured modulus, and macro-equivalent modulus around the skull. (B) 3D finite-element model of the skull and hyoid bone, with spatial variation of the Young's modulus in the skull. (C) First 10 modes of the skull under a pre-tension on the hyoid in the range 0–25 N. (D) Upper: stress wave at a brain location under impact direction. Lower: stress spectrum in the frequency domain obtained by FFT.

Several groups have investigated the mechanical behavior of the woodpecker using finite element modeling (FEM).<sup>26–32</sup> Generally, the models are based on the images obtained by X-ray computed tomography (CT) scans. The stress distribution caused by the impacts due to pecking is investigated. In some of these studies, the results are also compared with in vivo experiments, where the pecking force is measured by using force sensors and compared with that in other birds.<sup>27</sup> Zhu et al.<sup>31</sup> measured the Young's modulus of the skull, finding a periodic spatial variation, as reported in Figure 2A. Moreover, they performed a modal analysis on the skull by using FEM (Figure 2B) based on CT scan images and determining the first 10 natural frequencies, as shown in Figure 2C. The largest amplitude frequency components appear at 100 Hz and 8 kHz, which are well separated from the working frequency (around 20 Hz) and the natural frequencies (as derived in simulations), thus ensuring protection of the brain from injury.

Although results from different groups are not always in agreement, most researchers conclude that the shape of the skull, its microstructure, and its material composition are all relevant for the exceptional impact-attenuation properties in woodpeckers.<sup>10</sup> In particular, a grading in the bone porosity and mechanical properties is particularly important in damping high-frequency vibrations, which can be particularly harmful.<sup>33</sup> Many papers also point out the importance of the hyoid bone, very peculiar in woodpeckers, in the shock-absorption capability.<sup>34</sup> The hyoid is much longer than in other birds and wraps the skull as far as the eye sockets, forming a sort of safety belt around the skull. A specific study of the hyoid bone has been carried out by Jung et al.,<sup>34</sup> who

performed a macro- and micro-structural analysis of the hyoid apparatus and hyoid bones. The authors developed a 3D model of the

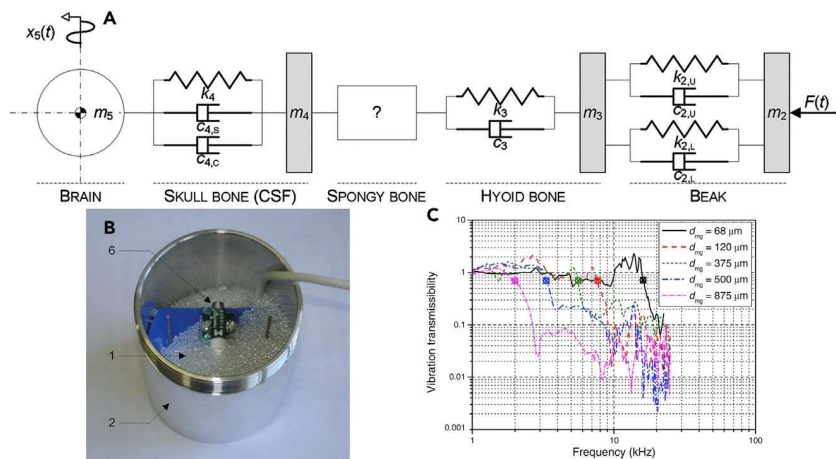


Figure 3. Modeling of vibration attenuation in the woodpecker skull (adapted from Yoon and Park<sup>10</sup>)  
 (A) Lumped-elements model of the head of a woodpecker.  
 (B) Empirical model of the spongy bone by means of an aluminum enclosure filled with glass microspheres.  
 (C) Vibration transmissibility as a function of frequency for different diameters of the SiO<sub>2</sub> microspheres.

hyoid and showed it to be formed by four main parts connected by three joints. Interestingly, by performing nanoindentation measurements, they also showed that it features a stiffer internal region surrounded by a softer, porous outer region, which could play an important role in dissipating the energy during pecking. Another important issue is the relative contribution of the upper and lower beaks in stress wave attenuation,<sup>27,35</sup> which is most probably dissipated through the body.<sup>32</sup>

Yoon and Park<sup>10</sup> showed that simple allometric scaling is not sufficient to explain the shock-absorbing properties of the woodpecker. Furthermore, they investigated its behavior by using a lumped element model including masses, springs, and dampers, as shown in Figure 3A. Given the difficulty in modeling the complexity of the sponge-like bone within the skull with lumped elements, the authors characterized its behavior by using an empirical method consisting of close-packed SiO<sub>2</sub> microglasses of different diameter (Figure 3B). The vibration transmissibility shows that the porous structure absorbs excitations with a higher frequency than a cutoff frequency, which is determined by the diameter of the glass microspheres, as reported in Figure 3C.

Lee et al.<sup>33</sup> reported a detailed analysis on the mechanical properties of the beak, showing that the keratin scales are more elongated than in other birds, and the waviness of the sutures between them is also higher than for other birds (1 for woodpecker, 0.3 for chicken, and 0.05 for toucan), most probably to favor energy dissipation due to the impact. Raut et al.<sup>36</sup> designed flexural waveguides with a sinusoidal depth variation inspired by the suture geometry of the woodpecker beak, which were tested by FEM analysis. The suture geometry helps to reduce the group speeds of the elastic wave propagation, whereas the presence of a viscoelastic material, as is the case for collagen in the beak sutures, significantly attenuates the wave amplitudes, suggesting a promising structure for applications in impact mitigation. Garland et al.<sup>37</sup> took inspiration from the same

mechanism of the sliding keratin scales in the beak to design friction metamaterials for energy adsorption.

### Seashells

Seashells are rigid biological structures that are considered to be ideally designed for mechanical protection, and they are now viewed as a source of inspiration in biomimetics.<sup>38,39</sup> A seashell is essentially a hard ceramic layer that covers the delicate tissues of mollusks. Many gastropod and bivalve shells have two layers: a calcite outer layer and an iridescent nacre inner layer. Calcite is a prismatic ceramic material composed of strong yet brittle calcium carbonate ( $\text{CaCO}_3$ ). Nacre, on the other hand, is a tough and pliable material that deforms significantly before collapsing.<sup>40</sup> It is considered that a protective structure that combines a hard layer on the surface with a tougher, more ductile layer on the interior optimizes impact-damping properties.<sup>39-41</sup> When a seashell is exposed to a concentrated load, such as a predator's bite, the hard ceramic covering resists penetration while the interior layer absorbs mechanical deformation energy. Overloading can cause the brittle calcite layer to fracture, causing cracks to spread into the soft tissue of the mollusk. Experiments have demonstrated that the thick nacreous layer can slow and eventually halt such fractures, delaying ultimate shell collapse. Although a significant amount of research has been performed on the structure and characteristics of nacre and calcite, there has been little research done on how these two materials interact in real shells. While there is evidence that nacre is tuned for toughness and energy absorption, little is known about how the shell structure fully utilizes its basic constituents, calcite and nacre.

One method employed to analyze the geometry of the shell at the macro scale, while accounting for the micromechanics of the nacreous layer, is to adopt multiscale modeling and optimization.<sup>39</sup> Different failure modes are possible depending on the geometry of the shell. On the other hand, according to optimization procedures, when two failure modes in different layers coincide, the shell performs best in avoiding sharp penetration. To reduce stress concentrations, the shell construction fully leverages the material's capabilities and distributes stress over two different zones. Furthermore, instead of converging to a single point, all parameters converge to a restricted range inside the design space.

According to the experiments done on two red abalone shells,<sup>39,42</sup> the actual seashell arranges its microstructure design to fully utilize its materials and delay failure, a result that is also obtained through optimization. The crack propagates over the thickness of the shell in three different failure situations. Furthermore, the seashell, which is constructed of standard ceramic material, can resist up to 1,900 N when loaded with a sharp indenter, which is an impressive load level given its size and structure.

### Suture joints

Suture joints with different geometries are commonly found in biology from micro to macro length scales (Figure 4A).<sup>43</sup> Examples include the carapace of the turtle,<sup>44,45</sup> the woodpecker beak,<sup>33</sup> the armored carapace of the box fish,<sup>8,46</sup> the cranium,<sup>47</sup> the seedcoat of *Portulaca oleracea*<sup>48</sup> and *Panicum miliaceum*,<sup>49</sup> the diatom *Ellerbeckia arenaria*,<sup>50</sup> and the ammonite fossil shells.<sup>51</sup>

In the aforementioned systems, the suture joint architecture, where different interdigitating stiff components, i.e., the teeth, are joined by a thin compliant seam, i.e., the interface layer, allows a high level of flexibility and is the key factor for the accomplishment of biological vital functions such as respiration, growth, locomotion, and

predatory protection.<sup>55-57</sup> Also, from a mechanical point of view, it has been demonstrated computationally and/or experimentally that this particular

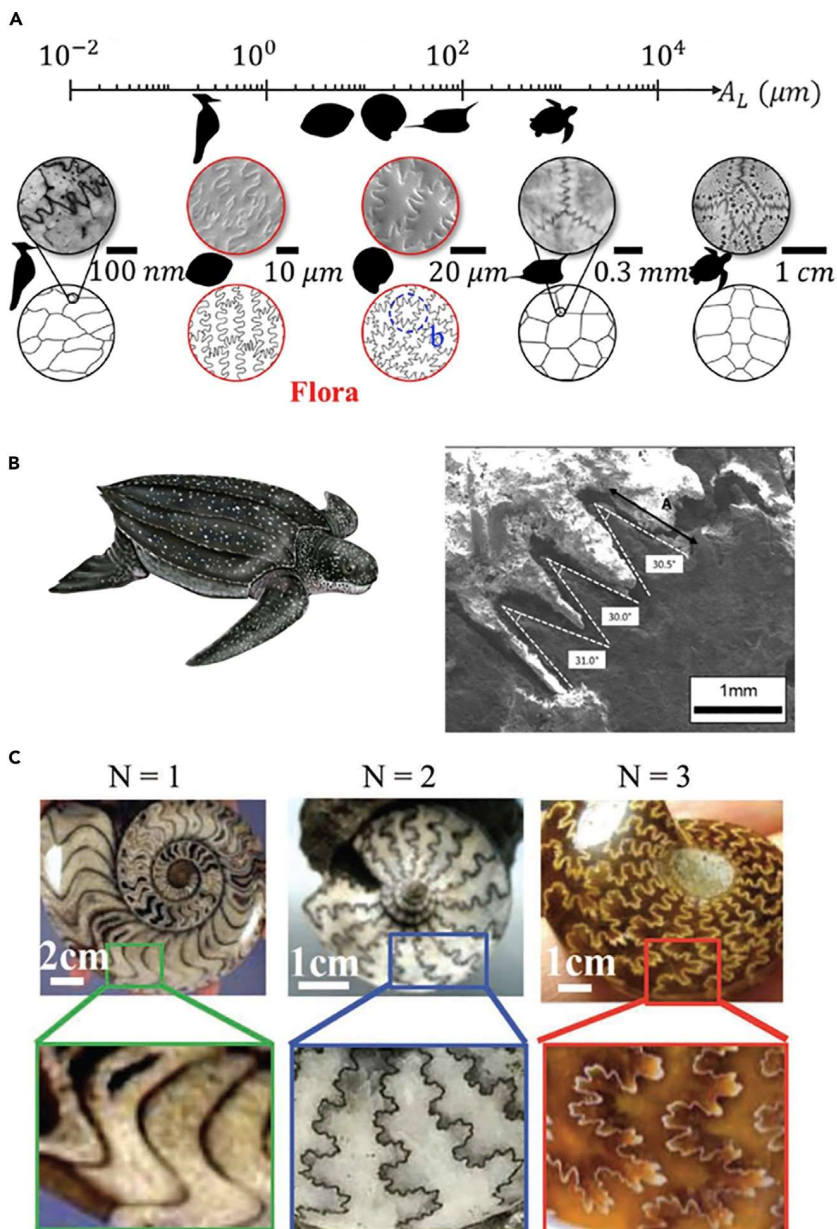


Figure 4. Biological systems with suture tessellation (A) Examples from flora and fauna (adapted from Gao and Li<sup>52</sup>).

(B) The leatherback turtle shell (adapted from Chen et al.<sup>53</sup>).

(C) Hierarchical sutures of increasing complexity found in ammonites (adapted from Studart<sup>54</sup>). configuration allows an excellent balance of stiffness, strength, toughness, and energy dissipation, and a more efficient way to bear and transmit loads.<sup>52,57-60</sup>

Several existing studies confirm this aspect,<sup>56,61</sup> where, in the case of cranial sutures, it emerges that an increased level of interdigitation, found among different mammalian species, leads to an increase in the suture's bending strength and energy storage. Emblematic is the case of the leatherback sea turtle (Figure 4B), a unique species of sea



turtle that has the capacity to dive to a depth of 1,200 m.<sup>53</sup> This is due to the particular design of the turtle's carapace, where an assemblage of bony plates interconnected with collagen fibers in a suture-like arrangement is covered by a soft and stretchable skin. As reported in Chen et al.,<sup>53</sup> the combination of these two elements provides a significant amount of flexibility under high hydrostatic pressure as well as exceptional mechanical functionality in terms of stiffness, strength, and toughness, the collagenous interfaces being an efficient crack arrester. In addition, De Blasio<sup>62</sup> explained not only how the high sinuosity and complexity of the suture lines in ammonites (Figure 4C) are the result of an evolutionary response to hydrostatic pressure but also that the stress, displacements, and deformations significantly decrease with the level of complexity. A similar result is also obtained in Pe' rez-Claros et al.,<sup>63</sup> who sought to clarify the functional significance of the complex suture pattern in ammonites.

### Bone

Bone has an extremely complex structure, encompassing seven levels of hierarchical organization, from nanocomposite mineralized collagen fibril upward.<sup>64</sup> Based on this building block, varying mineral contents and microstructure allow the construction of various types of tissue for different functionalities, e.g., withstanding tension, resisting impacts, and supporting bending and compression. Human cortical bone consists of cylindrical Haversian canals, each surrounded by multilayers of bone lamellae 10 mm thick, which have a rotated plywood structure in which mineralized collagen fibrils (100 nm in diameter) rotate from the transverse direction to the longitudinal direction across five sublayers. The fibrils are cemented together by extrafibrillar minerals and noncollagenous proteins.<sup>6</sup> Hierarchical structure plays a fundamental role in bone's exceptional mechanical properties. Bone's trabecular structure and hierarchy are responsible for its unmatched tensile strength, anisotropy, self-healing, and lightweight properties,<sup>64,65</sup> but also dynamic properties like impact damping.<sup>66,67</sup> Bioinspiration from bone structures has been exploited to seek enhanced static properties, strength, and toughness,<sup>68</sup> but relatively limited works have investigated it for dynamic applications. Ultrasonic wave measurements in bone to measure propagating velocity and attenuation have been performed for many years in various settings,<sup>69</sup> including "wet" bone,<sup>70</sup> showing that hydration is fundamental in defining dynamic properties. Studies in ultrasonics have typically focused on non-destructive evaluation of the bone structure.<sup>71,72</sup> It has also been shown that modal damping can be useful to detect bone integrity and osteoporosis,<sup>73</sup> also supported by ultrasonic wave propagation simulations in cancellous bone.<sup>74</sup> Dynamic measurement methods assessing modal damping have also been used to validate bone models.<sup>75</sup> In terms of bioinspiration, the porous structure of trabecular (rod- or truss-like structure) or velar bone (sail-like structure) is of particular interest because of its lightweight and impact-damping characteristics. Most of the work on such 3D frame structures<sup>76</sup> has addressed static properties.<sup>77</sup> However, recent articles have also addressed wave propagation<sup>78,79</sup> and impact loading.<sup>80</sup> Frame structures offer a convenient way to approximate trabeculae using truss-like structures, inspired by the well-known Bravais lattices.<sup>81</sup> The implementation of such lattices could pave the way to a simplified model of the bone structure, where the joints can be collapsed to point-like connections and the number of degrees of freedom can be drastically reduced.

### Attenuation of surface gravity waves by aquatic plants

If one considers damping of low-frequency vibrations over long timescales, one can look to natural barriers that allow prevention or delay of coastal erosion and the destruction of the corresponding habitats. One such example is the *Posidonia oceanica*, a flowering aquatic plant endemic to the Mediterranean Sea, which aggregates in large meadows, forming a Mediterranean habitat. This macrophyte has evolved by angiosperms typical of the intertidal zone and displays features similar to those of terrestrial plants: it has roots

and very flexible thin leaves of about 1-mm thickness and 1-cm width, without significant shape variations along the leaf length. The anchoring to sandy bottoms is provided by the horizontal growth of the rhizomes, which also grow vertically. The leaf length varies throughout the year because of the seasonal cycle and the marine climatic conditions and can vary between 0.3 m in winter and 1 m in summer.

The effects of seagrasses on unidirectional flows are well studied at different scales in the field and in laboratory flumes and numerical studies, while much less is known about the interaction between seagrass and waves. Wave attenuation due to *Posidonia* and flow conditions over and within vegetation fields has been investigated experimentally<sup>82</sup> and numerically.<sup>83</sup> It was found that the *Posidonia* is a good natural candidate for dissipating surface gravity waves in coastal regions. The study quantitatively assessed the physical value of the seagrass ecosystem restoration in this area, also opening new routes of action toward resilient, efficient, and sustainable solutions to coastal erosion. Natural barriers to water wave propagation other than vegetation such as the *Posidonia* exist and are fundamental. For example, ice covering the surface of the ocean around Antarctica and the Arctic Sea represents an important wave attenuation medium for slowing down the disintegration of the polar ice shelves. Quantitative measurements of such attenuation have been recently obtained through stereoscopic measurements.<sup>84</sup>

#### Attenuation of surface seismic waves by trees

Further recent evidence of natural barriers for large-scale vibrations is the attenuation of seismic surface waves achieved by trees.<sup>85</sup> The vibrations are transmitted to the trees through two coupling mechanisms, associated with two distinct vibrational modes. At high frequency (around 50 Hz), the longitudinal motion of the trees perpendicular to the soil surface is responsible for a high scattering effect on the surface wave and a hybridization to bulk shear waves. This means that the soil surface is mechanically blocked by the trees around those frequencies. In the low frequency range, below 1 Hz, the flexural motion of the trees induces different coupling effects on surface wave propagation. The flexural motion creates a bending moment at the soil/tree interface, which can create long-range coupling phenomena. Flexural resonances for the trees generally fall in the same frequency band as the micro-seismic noise produced by the ocean (between 0.3 and 0.8 Hz, detectable all over the world), which suggests a potential use of these frequencies to monitor the growth process of the trees and the evolution of their surrounding environment.<sup>86</sup>

#### Conclusions on impact-resistant structures

From the examples seen in the previous sections, it emerges that impact-resistant biological structures have a number of common features. The first is related to a complex hierarchical architecture spanning from the nano to the macro scale, as in the case of the woodpecker skull or suture joints. Hierarchy, in particular, allows the system to be multi-functional and to accomplish both biological and mechanical functions in an optimized fashion. Additionally, in terms of dynamical behavior, hierarchical structure allows the simultaneous addressing of various size scales and therefore frequency ranges. The second characteristic is heterogeneity, enabling natural materials to combine the desirable properties of their building blocks, which are typically light, widely occurring materials: polymeric and ceramic for mineralized systems or crystalline and amorphous phases for non-mineralized ones. Heterogeneity allows nature to create hierarchical composites that perform significantly better than the sum of their parts. Typically, the stiffer phase provides rigidity and strength, while the soft phase increases ductility. This distinctive quality leads, for example, to the exceptional impact-damping properties of the seashells described above. Another common trait of impact-resistant biological structures is

porosity, which plays an important role in dissipating impact energy and, at the same time, allows the overall weight of the system to decrease. Finally, the occurrence of complex geometrical features is a characteristic commonly found in impact-resistant structures in biology. The high sinuosity of the suture lines in ammonites and the helicoidal organization of the mantis shrimp's dactyl clubs are examples of this and provide direct evidence of their continually optimized nature, deriving from adaptation to the form that best achieves the required function.

## SENSING AND PREDATION

### Spider webs

Of all the natural structures that inspire and fascinate humankind, spider orb webs play a particularly central role and have been a source of interest and inspiration since ancient times. Spiders are able to make an extraordinary use of different types of silks to build webs that are the result of evolutionary adaptation and can deliver a compromise between many distinct requirements,<sup>87</sup> such as enabling trapping and localizing prey, detecting the presence of potential predators, and serving as channels for intra-specific communication.<sup>88</sup> The variety of structures, compositions, and functions has led to the development of a large amount of literature on spider silks and webs<sup>88–90</sup> and their possible bioinspired artificial counterparts.<sup>91,92</sup>

The overall mechanical properties of spider orb webs emerge from the interaction between at least five types of silk,<sup>3,93</sup> each with a distinct function in the web. The most important vibration-transmitting elements are made from the strong radial silk,<sup>94</sup> which also absorbs the kinetic energy of the prey,<sup>95,96</sup> while sticky spiral threads, covered with glue, are used to provide adhesion to retain the prey.<sup>97,98</sup> Moreover, junctions within the webs can be composed of two different types of silk:<sup>93</sup> the strong and stiff piriform silk, which provides strength to the anchorages<sup>99,100</sup> (Figures 5A and 5B), and the aggregate silk, which minimizes damage after impacts<sup>5,93</sup> (Figure 5C). The mechanical synergy of such systems is therefore due to the mechanical response of the junctions,<sup>101</sup> the constitutive laws of different types of silks, and the geometry of the webs.<sup>5</sup> The richness of these features, which is still the subject of many studies, has already inspired technologies with different goals in various scientific fields.<sup>102–104</sup>

Spider orb webs are able to stop prey while minimizing damage after impacts, thus maintaining their functionality,<sup>5</sup> partially exploiting the coupling with aerodynamic damping that follows prey impacts.<sup>96</sup> This makes orb webs efficient structures for capturing fast-moving prey,<sup>107</sup> whose location can then be detected because of the vibrational properties of the orb web. Efficiency in detecting prey by the spider is mediated by the transmission of signals in the web, which needs to carry sufficient information for the prey to be located.<sup>108</sup> Using laser vibrometry, it has been demonstrated that the radial threads are less prone to attenuating the propagation of the vibrations compared with the spirals,<sup>87</sup> because of their stiffer nature,<sup>109</sup> allowing them to efficiently transmit the entire frequency range from 1 to 10 kHz.

Spiral threads can undergo several types of motion, including transverse (perpendicular to both the thread and the plane of the web), lateral (perpendicular to the thread but in the plane of the web), and longitudinal (along with the thread axis), thus yielding complex frequency response characteristics.<sup>110–112</sup> Distinct wave speeds are also associated with each type of vibration; i.e., transverse wave speed is determined by string tension and mass density, while longitudinal wave speed is linked to

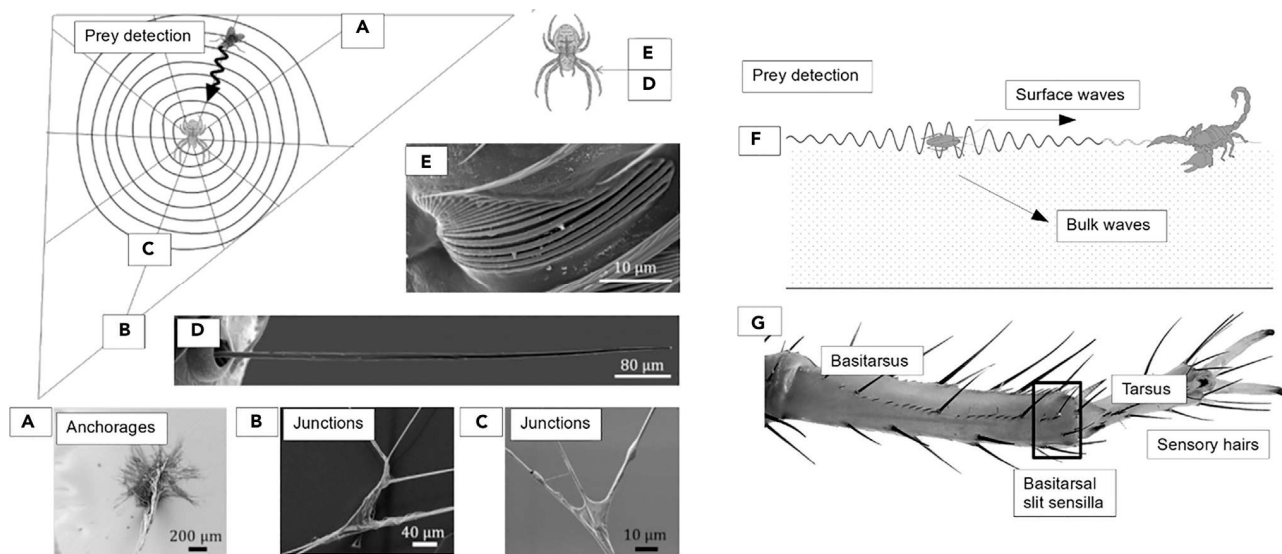


Figure 5. Prey-sensing similarities in spiders and scorpions

(A–E) (A) Web structure: a typical orb web of a spider *Nuctenea umbratica*. The web is built by means of junctions between threads and surfaces, (B) junctions between radial threads, (C) and junctions between radial and spiral threads. A flying prey can be eventually detected by air flow sensors, (D) the trichobothria. If the prey impacts the web, the vibrational signal will be transmitted mainly by radial threads and will be perceived by (E) lyriform organs of the spider. Figure adapted from Greco et al. and Ganske and Uhl.<sup>93,105</sup> (F) Schematic of scorpion prey detection using surface waves. (G) Sensory hairs and mechanoreceptors located at the slit sensilla sense surface waves. Adapted from Ganske et al.<sup>106</sup>

mass density and stiffness.<sup>113</sup> With the addition of more reinforcing threads because of the multiple lifeline addition by the spider, the orb webs appear to maintain signal transmission fidelity.<sup>114</sup> This provides further evidence of the impressive optimization achieved in these natural structures, which balances the trade-offs between structural and sensory functions.

The sonic properties of spider orb webs can also be significantly influenced by prestressing, as demonstrated in the study conducted by Mortimer et al.<sup>115</sup> Wirth and Barth<sup>116</sup> have shown that silk thread pre-stress increases with the mass of the spider, considering both inter- and intra-specific variations, and may be used to facilitate the sensing of smaller prey.<sup>117</sup> The pre-tension in webs can also be strongly influenced by large amplitude vibrations, as demonstrated by numerical analysis.<sup>118</sup> This dependence has been shown to be stronger if the structure is damaged, especially in the radial threads.<sup>119</sup>

Investigations on the vibration transmission properties of silk have been conducted by accessing its high-rate stress-strain behavior using ballistic impacts on *Bombyx mori* silk (which can be partially compared with spider silk).<sup>120</sup> Some studies have indicated that the capability of transmitting vibrations is relatively independent of environmental conditions such as humidity,<sup>121,122</sup> but in general it is expected that these conditions affect the silk's Young's modulus and the pre-stress level on the fibers and therefore the speed of sound (i.e., wave propagation speed) in the material.<sup>123–125</sup> This dependence is one of the reasons why the measurement of the speed of sound in silk has not produced homogeneous data<sup>111,126,127</sup> and could provide a possible degree of freedom for spiders in tuning the vibrational properties of their webs.<sup>115,126</sup>

Spider orb webs have proved to be one of the most inspiring systems to design structures able to manipulate elastic waves. Although many types of webs can be extremely efficient

in detecting and stopping prey,<sup>128</sup> plane structures tend to be preferred when it comes to bioinspired systems, because of their simplicity. Metamaterials can be designed to exploit the rich dynamic response and wave attenuation mechanism of orb webs,<sup>129</sup> based on locally resonant mechanisms to achieve band gaps in desired frequency ranges,<sup>130</sup> and further optimized to achieve advanced functionalities.<sup>131</sup> The possibility of designing low-frequency sound attenuators is also regarded as a common objective in metamaterials design, and spiderweb-inspired structures seem to be able to provide lightweight solutions to achieve this goal.<sup>132,133</sup>

### Spider sensing

Although many spiders have poor sight, remarkable sensors that make them capable of interacting with their surroundings have evolved,<sup>105</sup> including hair-shaped air movement detectors, tactile sensors, and thousands of extremely efficient strain detectors (lyriform organs such as slit sensilla) capable of transducing mechanical loads into nervous signals embedded in their exoskeletons.<sup>134–136</sup> Air flow sensors, named trichobothria (Figure 5D), seem to be specifically designed to perceive small air fluctuations induced by flying prey, which are detectable at a distance of several centimetres.<sup>137</sup> Spiders can process these signals in milliseconds and jump to catch the prey using only the information about air flow.<sup>138</sup> Although this could be sufficient to guide the detection of the prey using trichobothria, it could be that different hair-like structures undergo viscosity-mediated coupling that affects the perception efficiency. Interestingly, in the range of biologically relevant frequencies (30–300 Hz), viscous coupling of such hair-like structures is very small.<sup>139</sup> It seems, in particular, that the distance at which two structures do not interact is about 20–50 hair diameters, which is commonly found in nature.<sup>139,140</sup> Spiders are also equipped with strain sensors (lyriform organs), which are slits that occur isolated or in groups (Figure 5E), with a remarkable sensory threshold in terms of displacement (1.4–30 nm) and corresponding force stimulus (0.01 mN). Moreover, many of such organs have an exponential stiffening response to stimuli, which makes them suitable to detect a wide range of vibration amplitudes and frequencies. These organs act as filters with a typical high-pass behavior<sup>141</sup> to screen the environmental noise found in nature. Despite their remarkable capability in detecting vibration patterns (in frequencies between 0.1 Hz and several kHz), it is not yet clear how low-frequency signals are transmitted.<sup>142</sup> In any case, spider impact sensing on orb webs has been shown to be an intricate mechanism determined by both material properties and web structure.<sup>143</sup>

The sensing capabilities of spiders have driven the design of bioinspired solutions in terms of sensor technology. Materials scientists have designed bioinspired hair sensors that work both in air<sup>144,145</sup> and water.<sup>146</sup> Furthermore, the lyriform organs have inspired crack-based strain sensors,<sup>147,148</sup> eventually coupled with the mechanical robustness of spider silk.<sup>147</sup> Interestingly, these two types of structures (crack and hair sensors) may be combined in a multi-functional sensor. Results for such a spider-inspired ultrasensitive flexible vibration sensor demonstrated a sensitivity that outperforms many commercial counterparts.<sup>148</sup>

Spider silk threads are also capable of detecting airflows by means of their fluctuation,<sup>149</sup> providing an incredibly wide range of detectable frequencies, from 1 Hz to 50 kHz. Thus, by modifying these materials (e.g., making them conductive), it may be possible to produce devices able to expand the range of human hearing. It is clear, however, that many difficulties remain to be resolved to scale and fully optimize such bioinspired solutions. First, the reduction of the exposed surface can be large because of the need to integrate a sensor in the electronics. Second, wearing and application of the device could mechanically deteriorate its efficiency during its lifetime. Lastly, an engineering approach

is in stark contrast with biological ones. In this context, a profound breakthrough is needed to achieve high efficiency in the self-assembly of materials at the submicrometer scale.

#### Scorpion sensing

Scorpions are arachnids belonging to the subphylum Chelicerata of the arthropods (which includes spiders), which have evolved sensory mechanisms specially adapted to desertic environments.<sup>150</sup> Once structure-borne vibrations are produced in the ground, they propagate in the form of bulk and surface waves (Figure 5F): while the former propagate into the soil at large speeds and cannot be perceived by surface-dwelling animals, the latter can provide a useful information propagation channel for various species.<sup>151,152</sup> Sand offers an especially interesting medium in this regard; its wave speed and damping are significantly lower than in other soils, favoring time-domain discrimination and processing.<sup>153</sup> Brownell<sup>154</sup> has shown that two types of mechanoreceptors can be observed in the *Paruroctonus mesaensis* desert scorpion species (Figure 5G): (1) sensory hairs on the tarsus, which sense compressional waves, and (2) mechanoreceptors located at the slit sensilla, which sense surface waves, thus serving as the basis for the scorpion's perception of the target direction, performing a role of mechanotransduction similar to that observed in spiders.<sup>155</sup> Thus, these structures appear to be those responsible for vibration sensing in scorpions, even though some controversy exists regarding the use of other scorpion appendages for the same purpose.<sup>156</sup> Brownell and Farley have shown that this scorpion species can discriminate the vibration source direction by resolving the time difference in the activation of the slit sensilla mechano-receptors even for time intervals as small as 0.2 ms.<sup>157</sup> The same authors have also shown that, for short distances (down to 15 cm), scorpions can discriminate not only direction but also distance and vibration signal intensities, which are means to distinguish potential prey from potential predators.<sup>158</sup> Such underlying phenomena have been used to construct a numerical theory that simulates prey-localizing behavior in scorpions,<sup>159</sup> further motivating the development of artificial mechanisms based on this approach. Micro-structural investigations such as the ones performed by Wang et al.<sup>160</sup> have demonstrated that the slit sensilla owe their micro-vibration-sensing properties to their tessellated crackshaped slit microstructure,<sup>161</sup> further indicating that this type of microstructure can serve as a bioinspiration for the design of new mechano-sensing devices.<sup>147,162</sup>

#### Control of ground-borne sound by mammals

Vibration control in mammals is not restricted to airborne signals. Many use impacts by "drumming" parts of their bodies to generate vibrations that propagate in the soil. For example, foot-drumming patterns in rabbits and elephants are used to communicate with other individuals. Unlike in the cochlea, where the signal is split, and thus analyzed, according to its frequency content, foot drumming is based on the generation and analysis of complex transient vibrational patterns. One of the first species identified to use foot drumming to communicate is the blind rat.<sup>163</sup> More recent studies have identified the social and environmental monitoring purposes associated with this communication channel in elephants.<sup>164-166</sup>

#### Anti-predatory structures and strategies

It is thought that the origin of many distinctive morphological and/or behavioral traits of living organisms is related to the selective pressure exerted by

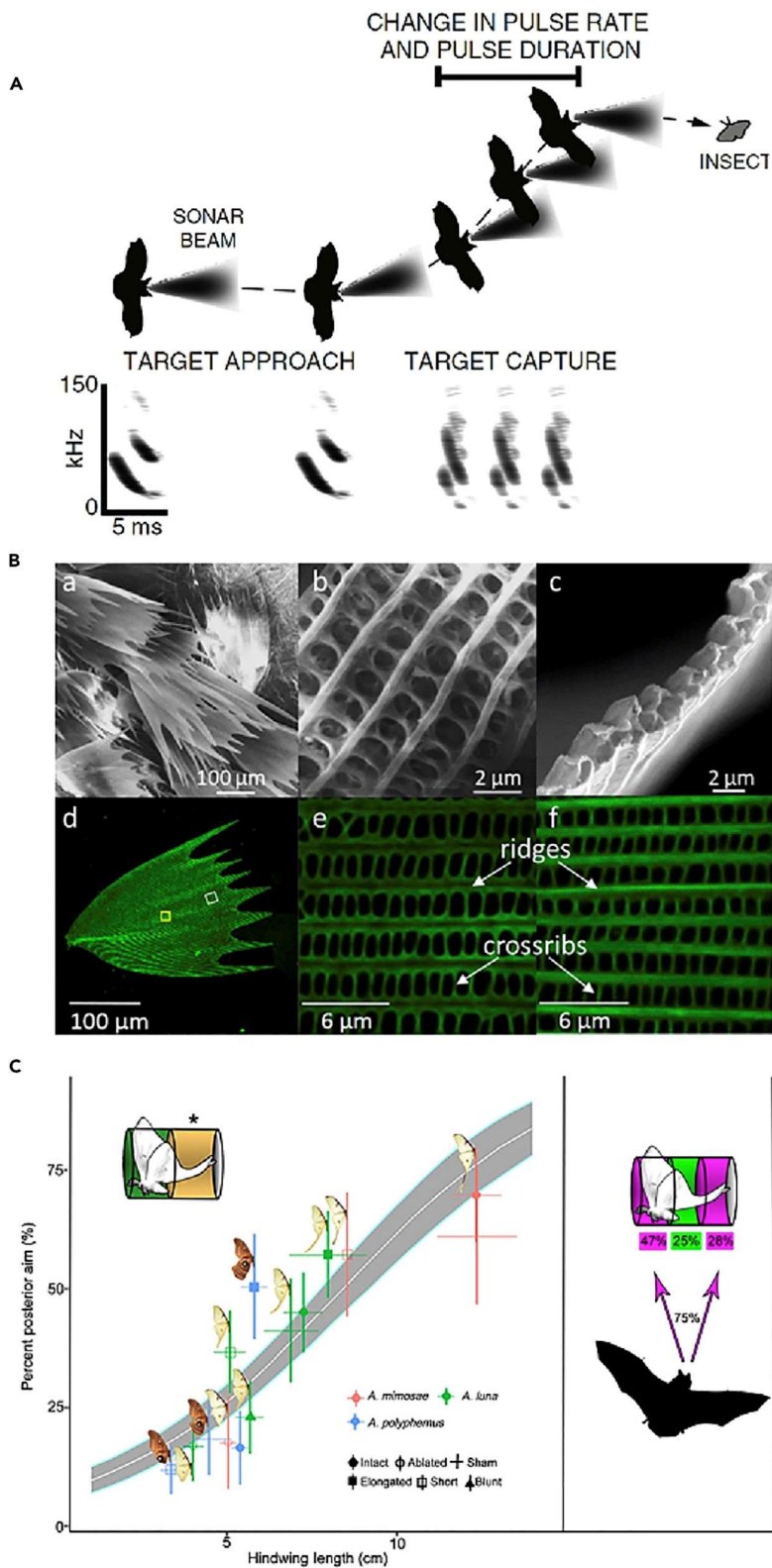


Figure 6. Anti-predatory strategies

(A–C) (A) The high-resolution 3D acoustic imaging system evolved by the echolocating bats (adapted from Wohlgenuth et al.<sup>177</sup>) and (B–C) the moth's strategies to avoid being detected: (B) the scale arrangement and structure at various size scales (adapted from Shen et al.<sup>178</sup>) and (C) hindwing tails. Behavioral analyses reveal that bats aim an increasing proportion of their attacks at the posterior half of the moth (indicated by yellow cylinder with asterisk) and that bats attacked the first and third sections of tailed moths 75% of the time, providing support

for the multipletarget illusion. An enlarged echo illusion would likely lead bats to target the hindwing just behind the abdomen of the moth, at the perceived echo center (highlighted in green); however, bats targeted this region only 25% of the time (adapted from Rubin et al.<sup>171</sup>). predators.<sup>167,168</sup> Generally, various defensive strategies can be adopted by organisms to reduce the probability of being attacked or, if attacked, to increase the chances of survival<sup>169</sup>. The first consists in avoiding detection (i.e., crypsis), through camouflage, masquerade, apostatic selection, subterranean lifestyle, or nocturnality, and deterring predators from attacking (i.e., aposematism) by displaying the presence of strong defenses or by signaling their threat by means of warning coloration, sounds, or odors.<sup>170</sup> The second is based on overpowering, outrunning, and diverting the assailants' strikes by creating sensory illusions to manipulate the predator's perception.<sup>171–173</sup>

Despite being extremely fascinating from an engineering point of view, the effectiveness of the first type of defensive strategies is restricted mainly to visual phenomena, and none of the strategies work on non-visually-oriented predators. However, although rare, some acoustic-based deflection strategies exist in nature. Most of them are related to one of the most famous examples of non-visually-oriented predators, i.e., echolocating bats (Figure 6A), which rely on echoes from their sonar cries to determine the position, size, and shape of moving objects in order to avoid obstacles and intercept prey in the environment.<sup>168,174–176</sup>

The first strategy to avoid detection by bats can be seen in some species of earless moth that, as a result of millions of years of evolution, developed a passive acoustic camouflage relying on a particular configuration of both the thorax and the wings. In particular, contrary to other species of moth that either evolved ears to detect the ultrasonic frequencies of approaching bats or produce, when under attack, ultrasound clicks to startle bats and alert them to the moth's toxicity,<sup>178–180</sup> the wings of earless moths are covered with an intricate layer of scales (Figure 6B) that serve as acoustic camouflage against bat echolocation.<sup>179,181</sup> According to O'Reilly et al.,<sup>179</sup> each leaf-shaped scale displays a hierarchical design, from the micro to the nano scale, consisting, at the larger scale, of two highly perforated laminae made of longitudinal ridges of nanometer size connected by a network of trabeculae pillars. This configuration leads to a highly porous structure that is able, because of the large proportion of interstitial honeycomb-like hollows, to absorb the ultrasound frequencies emitted by bats and thus reduce the amount of sound reflected back as echoes.<sup>182</sup> As a result, the moth partially disappears from the bat's biosonar and the distance at which the bat can detect the moth is reduced considerably,<sup>181</sup> representing a significant survival advantage. In addition, by exploring the vibrational behavior of a wing of a *Brunoa alcinoe* moth, researchers discovered not only that each scale behaves like a resonant ultrasound absorber, damping the first three resonances in the typical echolocation frequency range of bats,<sup>179</sup> but also that each has a different morphology and resonates at a particular frequency, creating a synergistically broadband absorption.<sup>182</sup> As reported in Neil et al.,<sup>182</sup> it can be said that the complex pattern of scales on moth wings exhibits the key features of a technological acoustic metamaterial.

Another example of an acoustic-based strategy to confuse predators is the long hindwing tail (Figure 6C) commonly found on luna moths (*Actias luna*). Such tails present a twist toward the end, and this distinguishing feature, as suggested in Barber et al.,<sup>183</sup> is the key to how the tail creates a sort of acoustic camouflage against echolocating bats. The tail, because of its length and twisted morphology, in reflecting the bat's sonar calls, produces two types of echoic sensory illusions.<sup>183</sup> The first consists in deflecting the bat's attacks from the vital parts of the body, i.e., head and thorax, to this inessential appendage. By



using high-speed infrared videography to analyze bat-moth interactions, according to the authors, in over half of the interactions, bats directed the attack at the moth's tail as the latter created an alternative target distracting from the principal one, i.e., the moth's body. Also, by comparing moths with the tail and moths with an ablated tail, a survival advantage of about 47% emerged.

The second sensory illusion provided by the twisted tail consists in inducing a misleading echoic target localization that confuses the hunting bats.<sup>171,183</sup> As reported in Barber et al.,<sup>183</sup> the origin of this effect is the twist located at the end of the tail, which creates a sequence of surfaces that have different orientations so that, independently of the inclination of both the incident sound waves and the fluttering moth, the tail is able to return an echo, complicating and spatially spreading the overall echoic response of the moth. In addition, the analysis of the overall acoustic return generated by the wings, body, and tail of a luna moth revealed an additional survival contribution of the twisted tail, consisting in a shift of the echoic target center, i.e., the center of the echo profile used by the bat to estimate the prey location, away from the moth's thorax.<sup>183</sup>

As previously mentioned, the second type of passive acoustic camouflage developed by earless moths consists in having much of the thorax covered by hairlike scales (Figure 7A) acting as a stealth coating against bat biosonar.<sup>184-186</sup> As suggested by Hegel and Casey<sup>186</sup> and Lee and Moss,<sup>187</sup> such thoracic scales create a dense layer of elongated piliform elements, resembling the lightweight fibrous materials used in engineering as sound insulators. Their potential as ultrasound absorbers was explored in Hegel and Casey<sup>186</sup> by means of tomographic echo images, and an average of 67% absorption of the impinging ultrasound energy emerged. Also, to provide a more in-depth investigation, the authors employed acoustic tomography to quantify the echo strength of diurnal butterflies, which are, contrary to moths, not a target for bat predation. The results were then used to establish a comparison with those derived for moths (Figure 7B). Interestingly, the analysis revealed that the absorptive performance is highly influenced by the scale thickness and density, with the very thin and less dense scales typical of butterflies able to absorb at most 20% of the impinging sound energy. Conversely, the denser and thicker moths' thorax scales possess ideal thickness values that allow the absorption of large amounts of bat ultrasonic calls. These findings are confirmed by Arenas and Crocker,<sup>184</sup> where an extended list of references is also provided.

Finally, airborne sound and vibration signals play an important role in bee communication and defense mechanisms.<sup>188</sup> The thorax of the bee contains a powerful musculature that is used to fly but also to produce vibratory impulses. For a long time, communication between bees seemed to be almost exclusively regulated by chemical signals, i.e., pheromones. In recent decades, it has become increasingly clear that bees live and interact in a world of sound and vibration.<sup>188,189</sup> One particular species, the Japanese bee *Vespa mandarinia japonica*,

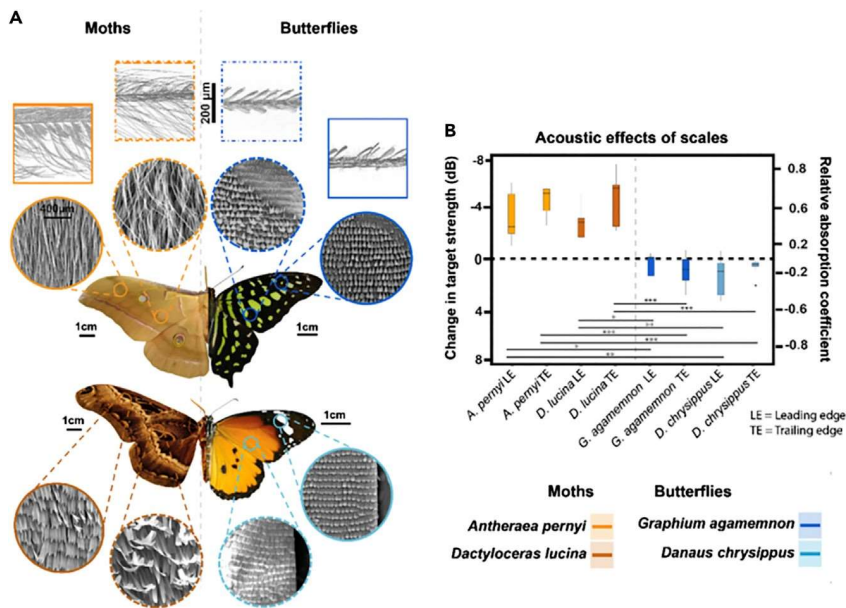


Figure 7. Tiling patterns and acoustic effects of lepidopteran scales  
 (A) SEM images of butterflies *Graphium agamemnon* and *Danaus chrysipus* and moths *Dactyloceras lucina* and *Antheraea pernyi*.  
 (B) Change in target strength caused by presence of scales, and equivalent intensity absorption coefficient (adapted from Neil et al.<sup>181</sup>).

uses sounds to coordinate and attack predators en masse. In particular, the defense mechanism developed by *V. mandarinia* relies on the control of dorsoventral and longitudinal muscles that do not contract alternately, as in flight, but tense simultaneously while the bee remains motionless. After a few minutes, the temperature of its thorax increases and can reach 43C (maximum temperature). If a foraging hornet tries to enter the hive, more than 500 workers quickly engulf it in a ball to rapidly raise the temperature to 47C, which is lethal for the hornet but not the bees.<sup>189</sup> This behavior is also associated with high neural activity, underlying the bees' computation for the use and production of sounds and vibrations.<sup>190</sup>

#### Conclusions on structures for sensing and predation

We have seen that structures that perform sensory functions are generally related to localization, allowing a certain species to either perceive surroundings, localize prey, or escape from predators. Some common and recurring features can be found. In all cases, the sensory capability of an organism benefits from specialized transducers used to detect vibrations (e.g., cuticles for insects and arachnids, silk for spiders). Interestingly, these transducers are often associated with nonlinear constitutive behavior; e.g., both cuticle<sup>191</sup> and silk<sup>192</sup> present a high stiffening behavior with an exponential constitutive law. Moreover, this relationship is strongly mediated by water content, which influences the properties of both the cuticle<sup>141,193</sup> and silk.<sup>194</sup> Thus, natural structures often present a strong relationship with a fluid or viscous medium as an agent capable of conferring specific mechanical properties. Generally speaking, the sensing capability is also strongly mediated by the interaction with the substrate (e.g., trees and leaves for spiders; sand and rocks for scorpions). Another common feature is that the interaction with the environment is also often mediated by air-flow sensors, with a common hairlike shape that is present in spiders,<sup>137</sup> scorpions,<sup>195</sup> crickets,<sup>196</sup> and fish.<sup>197</sup>

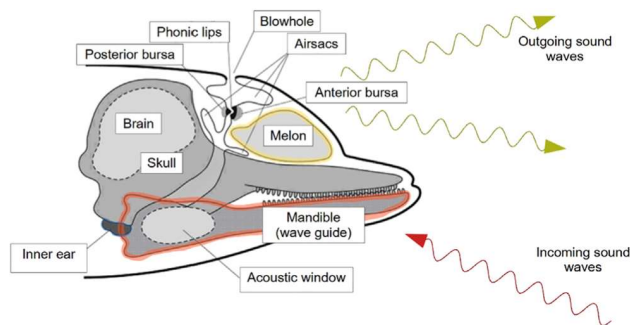


Figure 8. Structures for sound production and detection in dolphins  
 Modified and adapted from Cranford et al.<sup>215</sup>

## SOUND/VIBRATION CONTROL, FOCUSING, AND AMPLIFICATION

### Echolocation in odontocetes

Apart from communication purposes, toothed whales and dolphins (odontocetes) use clicks, sounds, and ultrasounds for sensing the surrounding environment, navigating, and locating prey.<sup>198</sup> This process is similar to that adopted by terrestrial animals like bats and is called echolocation.<sup>199–201</sup> The sounds are generated in special air cavities or sinuses in the head, can be emitted in a directional manner,<sup>202,203</sup> and their reflections from objects are received through the lower jaw and directed to the middle ear of the animal (Figure 8).<sup>204,205</sup> A number of studies have adopted CT scans and FEM to simulate sound generation and propagation in the heads of dolphins or whales, demonstrating how convergent sound beams can be generated and used to direct sound energy in a controlled manner, and also how sound reception can be directed through the lower jaw to the hearing organs.<sup>206,207</sup> Dible et al. have even suggested that the teeth in the lower jaw can act as a periodic array of scattering elements generating angular-dependent band gaps that can enhance the directional performance of the sensing process.<sup>208</sup> The emitted frequencies of the sounds used for echolocation are typically in the kHz range; e.g., bottlenose dolphins can produce directional, broadband clicks lasting less than a millisecond, centered between 40 and 130 kHz. Some studies have suggested that high-intensity focused sounds can even be used to disorient prey, although this remains to be confirmed.<sup>209,210</sup> The process of echolocation is extremely sensitive<sup>211,212</sup> and can provide odontocetes with a “3D view” of their surrounding environment. This is confirmed by the fact that sonar signals employed by military vessels can confuse and distress whales and dolphins, and even lead to mass strandings.<sup>213</sup> Reinwald et al.<sup>214</sup> envisaged that the capability, which is still poorly understood, of dolphins to accurately locate targets over a whole solid angle might be due to the correspondence between the reverberated coda of the signal transmitted along the bone to the ear and the location of the target that generated the signal.

### High-amplitude sound generation in mammals

An interesting mechanism exploited in nature to produce sounds is to develop specific resonating structures attached to the sound-producing organs of animals with the role to selectively filter out some frequencies and amplify others.<sup>216</sup> There are several examples of anatomical adaptations to increase sound radiation efficiency, such as air sacs in frogs,<sup>217</sup> birds,<sup>218</sup> and mammals<sup>219</sup> or enlarged larynges in howler monkeys<sup>220</sup> and hammerhead bats.<sup>221</sup> Some animals even change their environment by constructing horns or baffles that aid in radiating the sound.<sup>222</sup> The case of howler monkeys (*Alouatta*) is particularly interesting: these are widely considered to be the loudest land animals because their vocalizations can be heard clearly at a distance of 4.8 km. They emit sound at a level of 88 dB, which means 11 dB per kg, almost 10,000

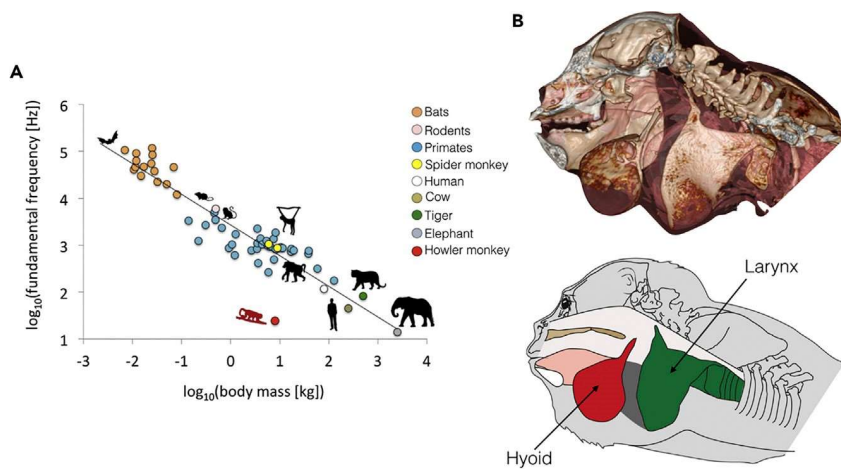


Figure 9. High-amplitude, low-frequency howler monkey communication (A) The exceptionally low frequency of howler monkey vocalizations. (B) Howler monkey vocal apparatus. Adapted from Dunn et al.<sup>220</sup>

times louder per unit mass compared with other animals (Figure 9A). The function of howling is thought to relate to intergroup spacing, territory protection, and social behavior, as well as possibly mate guarding.<sup>223</sup> The extraordinary capability of these monkeys to produce low frequencies and loud vocalizations has been largely studied, and the exact mechanism exploited is still debated.<sup>219</sup> However, two main elements are considered essential in this mechanism: expansion of the hyoid bone into a large shell-like organ in the throat and large hollow air sacs located on either side of the bone (Figure 9B). When the glottis produces low-frequency sounds, the hyoid and air sacs function as resonators, and the constrictions in the post-glottal structure (a narrow and curved supraglottal vocal tract) reduce the velocity of the air flow, elevating its pressure and, consequently, raising its volume.<sup>224</sup> The harshness of the roars is a result of the forced passage of air, resulting in irregular noisy vibrations. The acoustic function of the air sacs, however, is unclear, and not all authors agree on their function as resonators, proposing as an alternative an impedance-matching purpose<sup>225</sup> or potentially a resonance-suppressing one.<sup>226</sup>

#### Cochlea in mammals

The hearing organ in mammals has developed extraordinary capabilities from the point of view of the extension of audible frequencies and perceived intensities. The human ear (Figures 10A–10C), for example, is sensitive to eight octaves (20 Hz to 20 kHz) and is capable of distinguishing sounds within 12 orders of magnitude of intensity (120 dB). The evolutionary complexity of this organ has represented an obstacle to the deep understanding of all the mechanisms involved, and, even today, some aspects remain unexplained (for a review on the mechanical mechanisms involved, see Robles and Ruggiero<sup>227</sup> and Reichenbach and Hudspeth<sup>228</sup>). The cochlea (Figure 10E) is the core organ of the inner ear (in blue in Figure 10A), coiled in the form of a snail (hence its name) and enclosed by a bony shell. The cochlea is composed of two ducts, the scala vestibuli (SV) and scala tympani (ST) (see Figure 10B), filled with a liquid (perilymph) that is compressed by a membrane and hit by three miniscule bones of the middle ear (in red in Figure 10A). The pressure difference between the two ducts causes vibration in the basilar membrane, which separates them, and which conducts a largely independent traveling wave for each frequency component of the input (this mechanism was proposed for the first time in von Be'ke'sy and Peake<sup>229</sup> and then largely developed). However, because

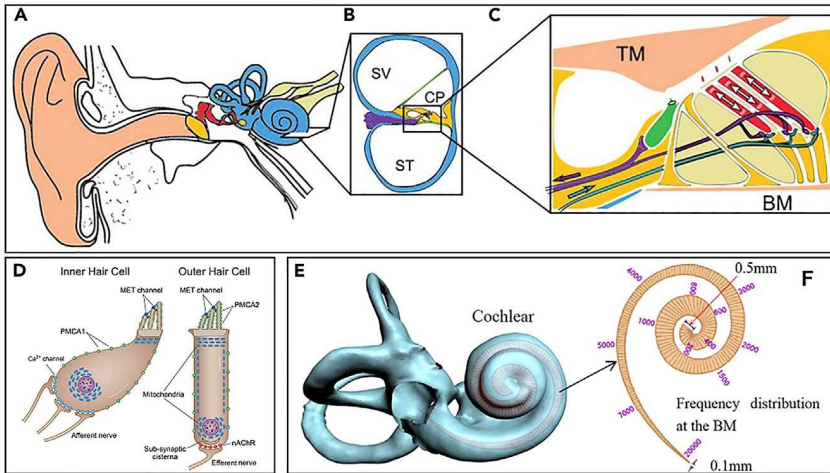


Figure 10. Cochlea structure

(A) The outer (beige), middle (red), and inner (blue) parts of the human ear.

(B–D) (B) Cross section of the cochlea showing the scala vestibuli (SV) and the scala tympani (ST), separated by the cochlear partition (CP), which contains the basilar membrane (BM) and the sensory hair cells (adapted from Rupin et al.<sup>232</sup>). These cells are represented in (C) in green (inner hair cells) and red (outer hair cells) and are also reported with more details in (D) (adapted from Fettiplace and Nam<sup>233</sup>).

(E) A 3D representation of the cochlea.

(F) Schematic map of the tonotopic property of the BM (adapted from Ma et al.<sup>234</sup>).

the basilar membrane is graded in mass and stiffness along its length,<sup>230</sup> each traveling wave grows in magnitude and decreases in wavelength until it peaks at a specific frequency-dependent position (see Figure 10F), thus allowing a spatial coding of the frequency contents. This is referred to as the tonotopic organization of the cochlea.<sup>231</sup> The mechanical vibration of the basilar membrane is then collected and translated into an electrical impulse from the hair cells (see Figure 10D) and sent to the brain for signal decoding.

One of the most relevant and studied characteristics of the basilar membrane is that its response to an external stimulus is highly nonlinear (i.e., not linearly proportional to the input amplitude), and this nonlinear response is also frequency specific. Moreover, each point of the cochlea has a different nonlinear response depending on the characteristic frequency relative to this specific point.<sup>235,236</sup> These features are especially evident in *in vivo* measurements, also underlining the existence of an active mechanism (otoacoustic emission) added to the merely mechanical ones (see, e.g., Kemp,<sup>237</sup> Ruggero et al.,<sup>238</sup> and Ren et al.<sup>239</sup>).

The mechanisms at play are complex, and often more than one possible explanation can be found in the literature, but different simplified models have tried to capture the basic features of the cochlea and reproduce its incredible capacity of sensing and its tonotopic and amplification behaviors (for a review see, e.g., De Boer<sup>240</sup> and Ni et al.<sup>241</sup>). One of the aspects that can be relevant for bioinspired applications in the propagation of elastic waves in solids is the influence of the geometry (spiral) on the frequency attenuation/loss and on the tonotopic property of the sample, as also pointed out by some works (see Manoussaki et al.<sup>242,243</sup>).

All these features attracted the interest of researchers working on mechanical and elastic wave manipulation devices, e.g., in the field of structural health monitoring,

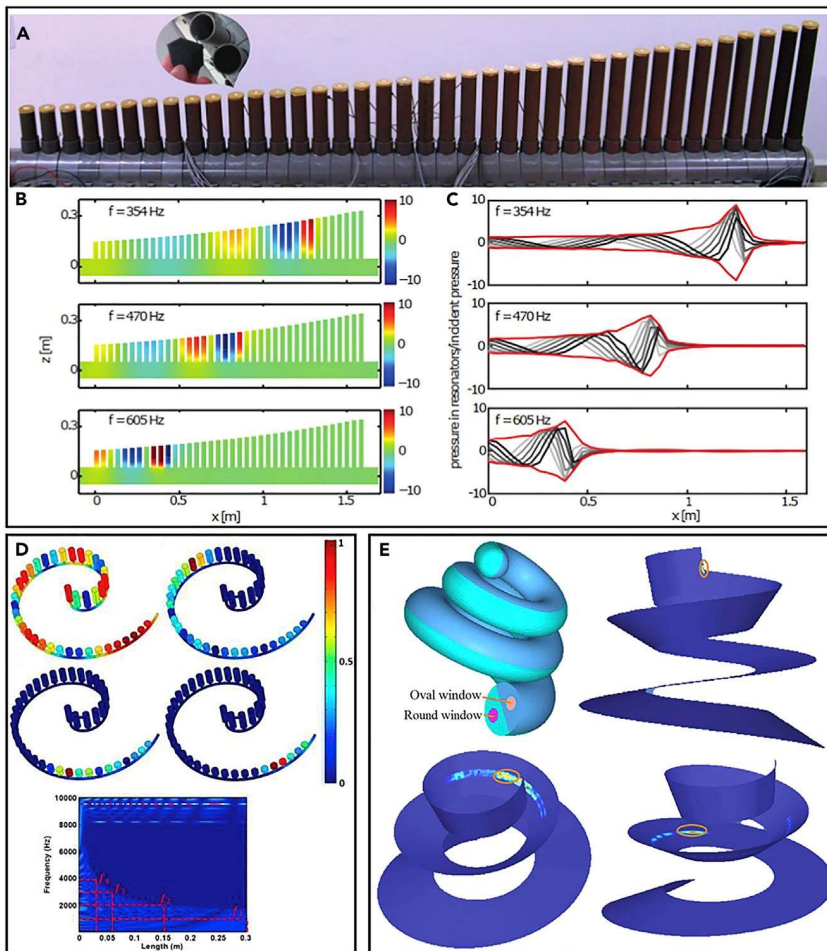


Figure 11. Metamaterial inspired by the cochlea

- (A) Gradient-index metamaterial for airborne sounds, made from 38 quarter-wavelength acoustic resonators of different heights.  
 (B) Corresponding simulated pressure field for 3 different frequencies.  
 (C) Spatial distribution of the acoustic pressure measured in the resonators for 3 single frequency excitations (adapted from Rupin et al.<sup>232</sup>).  
 (D) A rainbow trapper based on a set of Helmholtz resonators (adapted from Zhao and Zhou<sup>244</sup>). (E) A modal analysis of a helix model of cochlea, showing a different response to different frequency excitations (adapted from Ma et al.<sup>234</sup>).

sensor development, and guided waves. There are specific works in the literature that explicitly refer to the cochlea as a bioinspiration for metamaterial realizations and that propose acoustic rainbow sensors, where the aim is to separate different frequency components into different physical locations along the sensor (Figure 11).<sup>232,234,244,245</sup> In particular, the tonotopy and the low-amplitude amplifier are reproduced with a set of sub-wavelength active acoustic graded resonators, coupled to a main propagating waveguide in Rupin et al.<sup>232</sup> Similarly, based on a set of Helmholtz resonators arranged at sub-wavelength intervals along a cochlear-inspired spiral tube in Zhao and Zhou,<sup>244</sup> the authors realize an acoustic rainbow trapper that exploits the frequency-selective property of the structure to filter mechanical waves spectrally and spatially to reduce noise and interference in receivers. The tonotopy can also be obtained in a 3D model of the cochlea<sup>234</sup> by grading the mechanical parameters of a helicoidal membrane: in this case, the overall cochlea is a local resonant system with negative dynamic effective mass and stiffness.

Some of the examples of cochlea inspiration for the design of metamaterials are shown in Figure 11. In particular, in Figures 11A, 11B, and 11C, a gradient-index metamaterial for airborne sounds, made from 38 quarter-wavelength acoustic resonators of different heights, is reproduced (from Rupin et al.<sup>232</sup>). In Figure 11D, a rainbow trapper based on a set of Helmholtz resonators is described (from Zhao and Zhou<sup>244</sup>). In Figure 11E, a modal analysis of a helix model of a cochlea is reported, showing the different responses to different frequency excitations (in particular, at the top circle, the minimum natural frequency is 89.3 Hz, at the medial circle is 5,000.5 Hz, and at the base circle is 10,097.2 Hz).

## NATURAL STRUCTURAL EVOLUTION VERSUS OPTIMIZATION THROUGH ARTIFICIAL ALGORITHMS

The structures discussed in this review are the result of optimization processes due to natural evolution, spanning millions of years. Their common features are summarized in the sections “Conclusions on impact-resistant structures” and “Conclusions on structures for sensing and predation.” These evolutionary processes have, however, been constrained by the availability of material resources and their fabrication conditions. At the other end of the scale, there are fast-developing computational algorithms used in current technology that can be used to optimize artificial materials (often bioinspired) for similar goals where these boundary conditions can be relaxed or eliminated altogether. In artificial materials, the possibilities of design with different material combinations and distributions are virtually unbounded, and numerical algorithms can be used to optimize specific properties of nature-based architected structures.<sup>246</sup> The use of optimization techniques for the design of periodic structures able to attenuate vibrations, for instance, phononic crystals, aims to systematically achieve objectives such as maximizing absolute band gap widths,<sup>247</sup> normalized band gap width with respect to their central frequency,<sup>248,249</sup> or maximized attenuation per unit length.<sup>250</sup> For each given combination of materials, the objective function must be evaluated through the computation of the band structure of a given unit cell configuration, using various numerical methods.<sup>251–253</sup> A wide variety of optimization techniques to pursue the chosen objective are available in the literature. Among these, topology optimization is one of the most employed and well developed,<sup>254</sup> in combination with algorithms such as bidirectional evolutionary structural optimization.<sup>255</sup> Another common approach is the use of genetic algorithms, an optimization scheme that is a type of evolutionary algorithm<sup>256</sup> and is well suited for the design of phononic crystals.<sup>257</sup> Another possibility is the use of machine learning tools to design structures that present desirable characteristics, i.e., using an inverse approach.<sup>258</sup> Many of these approaches are being applied more and more in the field of phononics.<sup>259</sup> The types of optimized structures emerging from these algorithms have some common traits with naturally evolved structures and some distinctive differences. On the one hand, recurring features are many of those cited in the section “Conclusions on impact-resistant structures”: heterogeneity, porosity, hierarchical organization, efficient resonating structure, graded properties, and in some cases chirality.<sup>260,261</sup> In this case, artificial optimization techniques can improve existing bioinspired designs for specific objectives. On the other hand, implementing unconstrained numerical optimization can enable a wider exploration of the phase space, potentially leading to exotic designs with little resemblance to existing biological structures. However, this is not surprising because

optimization based on natural evolution is, in most cases, a multi-objective process, where different properties are simultaneously addressed (e.g., quasistatic strength/toughness and dynamic attenuation).

## CONCLUSIONS

We have presented a review of some notable examples of biological materials exhibiting optimized non-trivial structural architectures to achieve improved vibration control or elastic wave manipulation for many different purposes. The fields in which these features appear

are mainly impact and vibration damping and control, communication, prey detection or mimesis, and sound amplification and/or focusing. From the documented cases, some recurrent strategies and structural designs emerge. Among them, an important feature is hierarchical structure, which appears to be essential to enable effects at multiple scale levels and therefore in multiple frequency ranges. Moreover, these recurrent structural features appear at very different size scales (from micrometers to meters), in disparate environments (terrestrial or marine), and for different functions. This is an indication that the designs are particularly resilient and effective in their purposes, which encourages the adoption of a biomimetic approach to obtain the comparable types of optimized dynamic mechanical properties in artificial structures. This is a particularly attractive proposition in the field of phononic crystals and acoustic metamaterials, which have recently emerged as innovative solutions for wave manipulation and control and where a biomimetic approach to design has so far been limited to a few cases, especially considering that biological materials derive from self-assembly, so they are inherently periodic or hierarchical in structure. In general, further investigations in the natural world will no doubt continue to reveal original architectures, designs, and advanced functionalities to be exploited for metamaterials and other vibration-control technologies where function(s) can be achieved through form and structure.

## ACKNOWLEDGMENTS

All authors are supported by the European Commission H2020 FET Open Boheme grant no. 863179.

## AUTHOR CONTRIBUTIONS

Conceptualization, F.B. and N.M.P. All authors contributed to the writing of the manuscript.

## DECLARATION OF INTERESTS

The authors declare no competing interests.

## REFERENCES

- Ashby, M. (2010). *Materials Selection in Mechanical Design*, Fourth Edition (Butterworth-Heinemann), ISBN: 9780080952239.
- Ritchie, R.O. (2011). The conflicts between strength and toughness. *Nat. Mater.* 10, 817–822. <https://doi.org/10.1038/nmat3115>.
- Eisoldt, L., Smith, A., and Scheibel, T. (2011). Decoding the secrets of spider silk. *Mater. Today* 14, 80–86. [https://doi.org/10.1016/S1369-7021\(11\)70057-8](https://doi.org/10.1016/S1369-7021(11)70057-8).
- Wolff, J.O., Paterno, G.B., Liprandi, D., Ramirez, M.J., Bosia, F., van der Meijden, A., Michalik, P., Smith, H.M., Jones, B.R., Ravelo, A.M., et al. (2019). Evolution of aerial spider webs coincided with repeated structural optimization of silk anchorages. *Evolution* 73, 2122–2134. <https://doi.org/10.1111/evo.13834>.
- Cranford, S.W., Tarakanova, A., Pugno, N.M., and Buehler, M.J. (2012). Nonlinear material behaviour of spider silk yields robust webs. *Nature* 482, 72–76. <https://doi.org/10.1038/nature10739>.
- Wang, R., and Gupta, H.S. (2011). Deformation and fracture mechanisms of bone and nacre. *Annu. Rev. Mater. Res.* 41, 41–73. <https://doi.org/10.1146/annurev-matsci-062910-095806>.
- Gupta, H.S., Seto, J., Wagermaier, W., Zaslansky, P., Boesecke, P., and Fratzl, P. (2006). Cooperative deformation of mineral and collagen in bone at the nanoscale. *Proc. Natl. Acad. Sci. USA* 103, 17741–17746. <https://doi.org/10.1073/pnas.0604237103>.
- Yang, W., Chen, I.H., Gludovatz, B., Zimmermann, E.A., Ritchie, R.O., and Meyers, M.A. (2013). Natural flexible dermal armor. *Adv. Mater.* 25, 31–48. <https://doi.org/10.1002/adma.201202713>.
- Arndt, E.M., Moore, W., Lee, W.K., and Ortiz, C. (2015). Mechanistic origins of bombardier beetle (Brachinini) explosion-induced defensive spray pulsation. *Science* 348, 563–567. <https://doi.org/10.1126/science.1261166>.
- Yoon, S.H., and Park, S. (2011). A mechanical analysis of woodpecker drumming and its application to shock-absorbing systems. *Bioinspir. Biomim.* 6, 016003. <https://doi.org/10.1088/1748-3182/6/1/016003>.
- Sielmann, H. (1959). *My Year with the Woodpeckers* (Barrie and Rockliff). <https://books.google.it/books?id=jcHRxAEACAAJ>.
- Miniaci, M., Krushynska, A., Gliozzi, A.S., Kherraz, N., Bosia, F., and Pugno, N.M. (2018). Design and fabrication of bioinspired hierarchical dissipative elastic metamaterials. *Phys. Rev. Appl.* 10, 024012. <https://doi.org/10.1103/PhysRevApplied.10.024012>.
- Li, A., Zhao, X., Duan, G., Anderson, S., and Zhang, X. (2019). Diatom frustule-inspired metamaterial absorbers: the effect of hierarchical pattern arrays. *Adv. Funct. Mater.* 29, 1809029. <https://doi.org/10.1002/adfm.201809029>.
- Yan, G., Zou, H.X., Wang, S., Zhao, L.C., Wu, Z.Y., and Zhang, W.M. (2021). Bio-inspired vibration isolation: methodology and design. *Appl. Mech. Rev.* 73. <https://doi.org/10.1115/1.4049946>.
- Patek, S., Korff, W., and Caldwell, R. (2004). Biomechanics: deadly strike mechanism of a mantis shrimp. *Nature* 431, 82–85.
- Tadayon, M., Amini, S., Wang, Z., and Miserez, A. (2018). Biomechanical design of the Mantis shrimp saddle: a biomineralized spring used for rapid raptorial strikes. *iScience* 8, 271–282. <https://doi.org/10.1016/j.isci.2018.08.022>.



17. Tadayon, M., Amini, S., Masic, A., and Miserez, A. (2015). The Mantis shrimp saddle: a biological spring combining stiffness and flexibility. *Adv. Funct. Mater.* 25, 6437–6447. <https://doi.org/10.1002/adfm.201502987>.
18. Patek, S.N., and Caldwell, R.L. (2005). Extreme impact and cavitation forces of a biological hammer: strike forces of the peacock mantis shrimp *Odontodactylus scyllarus*. *J. Exp. Biol.* 208, 3655–3664. <https://doi.org/10.1242/jeb.01831>.
19. Weaver, J.C., Milliron, G.W., Miserez, A., Evans-Lutterodt, K., Herrera, S., Gallana, I., Mershon, W.J., Swanson, B., Zavattieri, P., DiMasi, E., and Kisailus, D. (2012). The stomatopod dactyl club: a formidable damage-tolerant biological hammer. *Science* 336, 1275–1280. <https://doi.org/10.1126/science.1218764>.
20. Chua, J.Q.I., Srinivasan, D.V., Idapalapati, S., and Miserez, A. (2021). Fracture toughness of the stomatopod dactyl club is enhanced by plastic dissipation: a fracture micromechanics study. *Acta Biomater.* 126, 339–349. <https://doi.org/10.1016/j.actbio.2021.03.025>.
21. Amini, S., Tadayon, M., Idapalapati, S., and Miserez, A. (2015). The role of quasi-plasticity in the extreme contact damage tolerance of the stomatopod dactyl club. *Nat. Mater.* 14, 943–950. <https://doi.org/10.1038/nmat4309>.
22. Taylor, J.R.A., and Patek, S.N. (2010). Ritualized fighting and biological armor: the impact mechanics of the mantis shrimp's telson. *J. Exp. Biol.* 213, 3496–3504. <https://doi.org/10.1242/jeb.047233>.
23. Taylor, J.R.A., Scott, N.I., and Rouse, G.W. (2019). Evolution of mantis shrimp telson armour and its role in ritualized fighting. *J. R. Soc. Interface* 16, 20190203. <https://doi.org/10.1098/rsif.2019.0203>.
24. Yaraghi, N.A., Trikanad, A.A., Restrepo, D., Huang, W., Rivera, J., Herrera, S., Zhernenkov, M., Parkinson, D.Y., Caldwell, R.L., Zavattieri, P.D., and Kisailus, D. (2019). The stomatopod telson: convergent evolution in the development of a biological shield. *Adv. Funct. Mater.* 29, 1902238. <https://doi.org/10.1002/adfm.201902238>.
25. Gibson, L.J. (2006). Woodpecker pecking: how woodpeckers avoid brain injury. *J. Zool.* 270, 462–465. <https://doi.org/10.1111/j.14697998.2006.00166.x>.
26. Oda, J., Sakamoto, J., and Sakano, K. (2006). Mechanical evaluation of the skeletal structure and tissue of the woodpecker and its shock absorbing system. *JSME Int. J. Ser. A* 49, 390–396. <https://doi.org/10.1299/jsmea.49.390>.
27. Wang, L., Cheung, J.T.M., Pu, F., Li, D., Zhang, M., and Fan, Y. (2011). Why do woodpeckers resist head impact injury: a biomechanical investigation. *PLoS One* 6, e26490. <https://doi.org/10.1371/journal.pone.0026490>.
28. Liu, Y., Qiu, X., Ma, H., Fu, W., and Yu, T.X. (2017). A study of woodpecker's pecking process and the impact response of its brain. *Int. J. Impact Eng.* 108, 263–271. <https://doi.org/10.1016/j.ijimpeng.2017.05.016>.
29. Wu, C.W., Zhu, Z.D., and Zhang, W. (2015). How woodpecker avoids brain injury? *J. Phys. Conf. Ser.* 628, 012007. <https://doi.org/10.1088/1742-6596/628/1/012007>.
30. Zhu, Z.D., Ma, G.J., Wu, C.W., and Chen, Z. (2012). Numerical study of the impact response of woodpecker's head. *AIP Adv.* 2, 042173. <https://doi.org/10.1063/1.4770305>.
31. Zhu, Z., Wu, C., and Zhang, W. (2014). Frequency analysis and anti-shock mechanism of woodpecker's head structure. *J. Bionic Eng.* 11, 282–287. [https://doi.org/10.1016/S1672-6529\(14\)60045-7](https://doi.org/10.1016/S1672-6529(14)60045-7).
32. Zhu, Z., Zhang, W., and Wu, C. (2014). Energy conversion in woodpecker on successive peckings and its role on anti-shock protection of brain. *Sci. China Technol. Sci.* 57, 1269–1275. <https://doi.org/10.1007/s11431-0145582-5>.
33. Lee, N., Horstemeyer, M.F., Rhee, H., Nabors, B., Liao, J., and Williams, L.N. (2014). Hierarchical multiscale structure - property relationships of the red-bellied woodpecker (*Melanerpes carolinus*) beak. *J. R. Soc. Interface* 11, 20140274. <https://doi.org/10.1098/rsif.2014.0274>.
34. Jung, J.Y., Naleway, S.E., Yaraghi, N.A., Herrera, S., Sherman, V.R., Bushong, E.A., Ellisman, M.H., Kisailus, D., and McKittrick, J. (2016). Structural analysis of the tongue and hyoid apparatus in a woodpecker. *Acta Biomater.* 37, 1–13. <https://doi.org/10.1016/j.actbio.2016.03.030>.
35. Li, Y., Zhang, W., Meng, Q.L., Jiang, G., and Wu, C.W. (2020). How woodpecker protects its brain from concussion during pecking compared with chicken and pigeon. *AIP Adv.* 10. <https://doi.org/10.1063/5.0004546>.
36. Raut, M.S., and Gopalakrishnan, S. (2021). Elastic and viscoelastic flexural wave motion in woodpecker-beak-inspired structures. *Bioinspir. Biomim.* 16. <https://doi.org/10.1088/1748-3190/abf745>.
37. Garland, A.P., Adstedt, K.M., Casias, Z.J., White, B.C., Mook, W.M., Kaehr, B., Jared, B.H., Lester, B.T., Leathe, N.S., Schwaller, E., and Boyce, B.L. (2020). Coulombic friction in metamaterials to dissipate mechanical energy. *Extreme Mech. Lett.* 40, 100847. <https://doi.org/10.1016/j.eml.2020.100847>.
38. Mayer, G. (2005). Rigid biological systems as models for synthetic composites. *Science* 310, 1144–1147. <https://doi.org/10.1126/science.1116994>.
39. Yourdkhani, M., Pasini, D., and Barthelat, F. (2010). The hierarchical structure of seashells optimized to resist mechanical threats. *WIT Trans. Ecol. Environ.* 138. <https://doi.org/10.2495/DN100131>.
40. Barthelat, F., Tang, H., Zavattieri, P., Li, C., and Espinosa, H. (2007). On the mechanics of mother-of-pearl: a key feature in the material hierarchical structure. *J. Mech. Phys. Solids* 55, 306–337. <https://doi.org/10.1016/j.jmps.2006.07.007>.

41. Sarikaya, M., and Aksay, I.A. (1995). *Biomimetics: Design and Processing of Materials* (AIP Series in Polymers and Complex Materials) (American Institute of Physics).
42. Meyers, M.A., Lin, A.Y.M., Chen, P.Y., andMuyco, J. (2008). Mechanical strength of abalone nacre: role of the soft organic layer. *J. Mech. Behav. Biomed. Mater.* 1, 76–85. <https://doi.org/10.1016/j.jmbbm.2007.03.001>.
43. Barthelat, F., Yin, Z., and Buehler, M.J. (2016). Structure and mechanics of interfaces in biological materials. *Nat. Rev. Mater.* 1, 16007. <https://doi.org/10.1038/natrevmats.2016.7>.
44. Krauss, S., Monsonego-Ornan, E., Zelzer, E.,Fratzl, P., and Shahar, R. (2009). Mechanical function of a complex three-dimensional suture joining the bony elements in the shell of the red-eared slider turtle. *Adv. Mater.* 21, 407–412. <https://doi.org/10.1002/adma.200801256>.
45. Damiens, R., Rhee, H., Hwang, Y., Park, S.J.,Hammi, Y., Lim, H., and Horstemeyer, M.F. (2012). Compressive behavior of a turtle’s shell: experiment, modeling, and simulation. *J. Mech. Behav. Biomed. Mater.* 6, 106–112. <https://doi.org/10.1016/j.jmbbm.2011.10.011>.
46. Yang, W., Naleway, S.E., Porter, M.M.,Meyers, M.A., and McKittrick, J. (2015). The armored carapace of the boxfish. *Acta Biomater.* 23, 1–10. <https://doi.org/10.1016/j.actbio.2015.05.024>.
47. Pritchard, J.J., Scott, J.H., and Girgis, F.G. (1956). The structure and development of cranial and facial sutures. *J. Anat.* 90, 73–86.
48. Gao, C., Hasseldine, B.P.J., Li, L., Weaver,J.C., and Li, Y. (2018). Amplifying strength, toughness, and auxeticity via wavy sutural tessellation in plant seedcoats. *Adv. Mater.* 30, e1800579. <https://doi.org/10.1002/adma.201800579>.
49. Lu, H., Zhang, J., Wu, N., Liu, K.B., Xu, D., andLi, Q. (2009). Phytoliths analysis for the discrimination of Foxtail millet (*Setaria italica*) and Common millet (*Panicum miliaceum*). *PLoS One* 4, e4448. <https://doi.org/10.1371/journal.pone.0004448>.
50. Gebeshuber, I.C., Kindt, J.H., Thompson, J.B., Del Amo, Y., Stachelberger, H., Brzezinski, M.A., Stucky, G.D., Morse, D.E., and Hansma, P.K. (2003). Atomic force microscopy study of living diatoms in ambient conditions. *J. Microsc.* 212, 292–299. <https://doi.org/10.1111/j.1365-2818.2003.01275.x>.
51. Li, Y., Ortiz, C., and Boyce, M.C. (2012). Bioinspired, mechanical, deterministic fractal model for hierarchical suture joints. *Phys. Rev. E Stat. Nonlin. Soft Matter Phys.* 85, 031901. <https://doi.org/10.1103/PhysRevE.85.031901>.
52. Gao, C., and Li, Y. (2019). Mechanical modelof bio-inspired composites with sutural tessellation. *J. Mech. Phys. Solids* 122, 190–204. <https://doi.org/10.1016/j.jmps.2018.09.015>.
53. Chen, I.H., Yang, W., and Meyers, M.A. (2015). Leatherback sea turtle shell: a tough and flexible biological design. *Acta Biomater.* 28, 2–12. <https://doi.org/10.1016/j.actbio.2015.09.023>.
54. Studart, A.R. (2012). Towards highperformance bioinspired composites. *Adv. Mater.* 24, 5024–5044. <https://doi.org/10.1002/adma.201201471>.
55. Jaslow, C.R., and Biewener, A.A. (1995). Strainpatterns in the horncores, cranial bones and sutures of goats (*Capra hircus*) during impact loading. *J. Zool.* 235, 193–210. <https://doi.org/10.1111/j.1469-7998.1995.tb05137.x>.
56. Jaslow, C.R. (1990). Mechanical propertiesof cranial sutures. *J. Biomech.* 23, 313–321. [https://doi.org/10.1016/00219290\(90\)90059-C](https://doi.org/10.1016/00219290(90)90059-C).
57. Li, Y., Ortiz, C., and Boyce, M.C. (2013). Ageneralized mechanical model for suture interfaces of arbitrary geometry. *J. Mech. Phys. Solids* 61, 1144–1167. <https://doi.org/10.1016/j.jmps.2012.10.004>.
58. Yu, Z., Liu, J., and Wei, X. (2020). Achievingoutstanding damping performance through bio-inspired sutural tessellations. *J. Mech. Phys. Solids* 142, 104010. <https://doi.org/10.1016/j.jmps.2020.104010>.
59. Gao, C., Slesarenko, V., Boyce, M.C., Rudykh,S., and Li, Y. (2018). Instability-induced pattern transformation in soft metamaterial with hexagonal networks for tunable wave propagation. *Sci. Rep.* 8, 11834. <https://doi.org/10.1038/s41598-018-30381-1>.
60. Ghazlan, A., Ngo, T.D., and Tran, P. (2015). Influence of interfacial geometry on the energy absorption capacity and load sharing mechanisms of nacreous composite shells. *Compos. Struct.* 132, 299–309. <https://doi.org/10.1016/j.compstruct.2015.05.045>.
61. Jasinowski, S.C., Reddy, B.D., Louw, K.K., andChinsamy, A. (2010). Mechanics of cranial sutures using the finite element method. *J. Biomech.* 43, 3104–3111. <https://doi.org/10.1016/j.jbiomech.2010.08.007>.
62. De Blasio, F.V. (2008). The role of suturecomplexity in diminishing strain and stress in ammonoid phragmocones. *Lethaia* 41, 15–24. <https://doi.org/10.1111/j.1502-3931.2007.00037.x>.
63. Pe´rez-Claros, J.A., Palmqvist, P., and Olo´ riz, F. (2002). First and second orders of suture complexity in ammonites: a new methodological approach using fractal analysis. *Math. Geol.* 34. <https://doi.org/10.1023/A:1014847007351>.
64. Currey, J.D. (2013). *Bones: Structure and Mechanics* (Princeton University Press), ISBN: 9781400849505.
65. Sullivan, T.N., Wang, B., Espinosa, H.D., andMeyers, M.A. (2017). Extreme lightweight structures: avian feathers and bones. *Mater. Today* 20, 377–391. <https://doi.org/10.1016/j.mattod.2017.02.004>.
66. Qwamizadeh, M., Liu, P., Zhang, Z., Zhou, K.,and Wei Zhang, Y. (2016). Hierarchical structure enhances and tunes the damping behavior of load-bearing biological materials. *J. Appl. Mech.* 83. <https://doi.org/10.1115/1.4032861>.

67. Lazarus, B.S., Velasco-Hogan, A., Go' mez-del Ri' o, T., Meyers, M.A., and Jasiuk, I. (2020). A review of impact resistant biological and bioinspired materials and structures. *J. Mater. Res. Technol.* 9, 15705–15738. <https://doi.org/10.1016/j.jmrt.2020.10.062>.
68. Libonati, F., and Buehler, M.J. (2017). Advanced structural materials by bioinspiration. *Adv. Eng. Mater.* 19, 1600787. <https://doi.org/10.1002/adem.201600787>.
69. Evans, J.A., and Tavakoli, M.B. (1990). Ultrasonic attenuation and velocity in bone. *Phys. Med. Biol.* 35, 1387–1396. <https://doi.org/10.1088/0031-9155/35/10/004>.
70. Lakes, R., Yoon, H.S., and Katz, J.L. (1986). Ultrasonic wave propagation and attenuation in wet bone. *J. Biomed. Eng.* 8, 143–148. [https://doi.org/10.1016/01415425\(86\)90049-X](https://doi.org/10.1016/01415425(86)90049-X).
71. Hai' at, G., Padilla, F., Peyrin, F., and Laugier, P. (2008). Fast wave ultrasonic propagation in trabecular bone: numerical study of the influence of porosity and structural anisotropy. *J. Acoust. Soc. Am.* 123, 1694–1705. <https://doi.org/10.1121/1.2832611>.
72. Bochud, N., Vallet, Q., Minonzio, J.G., and Laugier, P. (2017). Predicting bone strength with ultrasonic guided waves. *Sci. Rep.* 7, 43628. <https://doi.org/10.1038/srep43628>.
73. Panteliou, S.D., Xirafaki, A.L., Panagiotopoulos, E., Varakis, J.N., Vagenas, N.V., and Kontoyannis, C.G. (2004). Modal damping for monitoring bone integrity and osteoporosis. *J. Biomech. Eng.* 126, 1–5. <https://doi.org/10.1115/1.1644561>.
74. Michimoto, I., Miyashita, K., Suzuyama, H., Yano, K., Kobayashi, Y., Saito, K., and Matsukawa, M. (2021). Simulation study on the effects of cancellous bone structure in the skull on ultrasonic wave propagation. *Sci. Rep.* 11, 17592. <https://doi.org/10.1038/s41598-021-96502-5>.
75. Neupetsch, C., Hensel, E., Werner, M., Meißner, S., Troge, J., Drossel, W.G., and Rotsch, C. (2019). Development and validation of bone models using structural dynamic measurement methods. *Curr. Dir. Biomed. Eng.* 5, 343–345. <https://doi.org/10.1515/cdbme-2019-0086>.
76. Kadic, M., Milton, G.W., van Hecke, M., and Wegener, M. (2019). 3D metamaterials. *Nat. Rev. Phys.* 1, 198–210. <https://doi.org/10.1038/s42254-018-0018-y>.
77. Meza, L.R., Philipot, G.P., Portela, C.M., Maggi, A., Montemayor, L.C., Comella, A., Kochmann, D.M., and Greer, J.R. (2017). Reexamining the mechanical property space of three-dimensional lattice architectures. *Acta Mater.* 140, 424–432. <https://doi.org/10.1016/j.actamat.2017.08.052>.
78. Arretche, I., and Matlack, K.H. (2019). Experimental testing of vibration mitigation in 3D-printed architected metastructures. *J. Appl. Mech.* 86. <https://doi.org/10.1115/1.4044135>.
79. Zelhofer, A.J., and Kochmann, D.M. (2017). On acoustic wave beaming in two-dimensional structural lattices. *Int. J. Solids Struct.* 115–116, 248–269. <https://doi.org/10.1016/j.ijsostr.2017.03.024>.
80. Aguirre, T.G., Fuller, L., Ingrole, A., Seek, T.W., Wheatley, B.B., Steineman, B.D., Donahue, T.L.H., and Donahue, S.W. (2020). Bioinspired material architectures from bighorn sheep homocore velar bone for impact loading applications. *Sci. Rep.* 10, 18916. <https://doi.org/10.1038/s41598-020-76021-5>.
81. Jones, H. (1957). Introduction to solid state physics by C. Kittel. *Acta Crystallogr.* 10, 390. <https://doi.org/10.1107/s0365110x57001280>.
82. Stratigaki, V., Manca, E., Prinos, P., Losada, I.J., Lara, J.L., Sclavo, M., Amos, C.L., Ca'ceres, I., and Sa' nchez-Arcilla, A. (2011). Large-scale experiments on wave propagation over *Posidonia oceanica*. *J. Hydraul. Res.* 49, 31–43. <https://doi.org/10.1080/00221686.2011.583388>.
83. Novi, L. (2019). A Numerical Model for High Resolution Simulations of Marine Fluid Dynamics and Coastal Morphodynamics (Univ Pisa.). PhD Thesis.
84. Alberello, A., Bennetts, L., Onorato, M., Vichi, M., MacHutchon, K., Eayrs, C., Ntamba Ntamba, B., Benetazzo, A., Bergamasco, F., Nelli, F., et al. (2022). Three-dimensional imaging of waves and floe sizes in the marginal ice zone during an explosive cyclone. Preprint at arXiv. <https://doi.org/10.48550/arXiv.2103.08864>.
85. Lott, M., Roux, P., Garambois, S., Gue' guen, P., and Colombi, A. (2019). Evidence of metamaterial physics at the geophysics scale: the METAFORÉ experiment. *Geophys. J. Int.* 220. <https://doi.org/10.1093/gji/ggz528>.
86. Moore, J.R., and Maguire, D.A. (2004). Natural sway frequencies and damping ratios of trees: concepts, review and synthesis of previous studies. *Trees* 18, 195–203. <https://doi.org/10.1007/s00468-003-0295-6>.
87. Masters, W.M., and Markl, H. (1981). Vibration signal transmission in spider orb webs. *Science* 213, 363–365. <https://doi.org/10.1126/science.213.4505.363>.
88. Eberhard, W. (2020). *Spider Webs* (University of Chicago Press), pp. 24–74. <https://doi.org/10.7208/9780226534749-002>.
89. Asakura, T., and Miller, T. (2014). *Biotechnology of Silk* (Springer).
90. Basu, A. (2015). *Advances in Silk Science and Technology* (Woodhead Publishing).
91. Rising, A., and Johansson, J. (2015). Toward spinning artificial spider silk. *Nat. Chem. Biol.* 11, 309–315. <https://doi.org/10.1038/nchembio.1789>.
92. Andersson, M., Jia, Q., Abella, A., Lee, X.Y., Landreh, M., Purhonen, P., Hebert, H., Tenje, M., Robinson, C.V., Meng, Q., et al. (2017). Biomimetic spinning of artificial spider silk from a chimeric minispidroin. *Nat. Chem. Biol.* 13, 262–264. <https://doi.org/10.1038/nchembio.2269>.

93. Greco, G., Pantano, M.F., Mazzolai, B., and Pugno, N.M. (2019). Imaging and mechanical characterization of different junctions in spider orb webs. *Sci. Rep.* 9, 5776. <https://doi.org/10.1038/s41598-019-42070-8>.
94. Agnarsson, I., Kuntner, M., and Blackledge, T.A. (2010). Bioprospecting finds the toughest biological material: extraordinary silk from a giant riverine orb spider. *PLoS One* 5, e11234. <https://doi.org/10.1371/journal.pone.0011234>.
95. Yu, H., Yang, J., and Sun, Y. (2015). Energy absorption of spider orb webs during prey capture: a mechanical analysis. *J. Bionic Eng.* 12, 453–463. [https://doi.org/10.1016/S16726529\(14\)60136-0](https://doi.org/10.1016/S16726529(14)60136-0).
96. Sensenig, A.T., Lorentz, K.A., Kelly, S.P., and Blackledge, T.A. (2012). Spider orb webs rely on radial threads to absorb prey kinetic energy. *J. R. Soc. Interface* 9, 1880–1891. <https://doi.org/10.1098/rsif.2011.0851>.
97. Guo, Y., Chang, Z., Guo, H.Y., Fang, W., Li, Q., Zhao, H.P., Feng, X.Q., and Gao, H. (2018). Synergistic adhesion mechanisms of spider capture silk. *J. R. Soc. Interface* 15, 20170894. <https://doi.org/10.1098/rsif.2017.0894>.
98. Sahni, V., Blackledge, T.A., and Dhinojwala, A. (2011). Changes in the adhesive properties of spider aggregate glue during the evolution of cobwebs. *Sci. Rep.* 1, 41. <https://doi.org/10.1038/srep00041>.
99. Grawe, I., Wolff, J.O., and Gorb, S.N. (2014). Composition and substrate-dependent strength of the silken attachment discs in spiders. *J. R. Soc. Interface* 11, 20140477. <https://doi.org/10.1098/rsif.2014.0477>.
100. Wolff, J.O., and Herberstein, M.E. (2017). Three-dimensional printing spiders: back-and-forth glue application yields silk anchorages with high pull-off resistance under varying loading situations. *J. R. Soc. Interface* 14, 20160783. <https://doi.org/10.1098/rsif.2016.0783>.
101. Meyer, A., Pugno, N.M., and Cranford, S.W. (2014). Compliant threads maximize spider silk connection strength and toughness. *J. R. Soc. Interface* 11, 20140561. <https://doi.org/10.1098/rsif.2014.0561>.
102. Zhu, Q., Tang, X., Feng, S., Zhong, Z., Yao, J., and Yao, Z. (2019). ZIF-8@SiO<sub>2</sub> composite nanofiber membrane with bioinspired spider web-like structure for efficient air pollution control. *J. Memb. Sci.* 581, 252–261. <https://doi.org/10.1016/j.memsci.2019.03.075>.
103. Xu, B., Yang, Y., Yan, Y., and Zhang, B. (2019). Bionics design and dynamics analysis of space webs based on spider predation. *Acta Astronaut.* 159, 294–307. <https://doi.org/10.1016/j.actaastro.2019.03.045>.
104. Vollrath, F., and Krink, T. (2020). Spider webs inspiring soft robotics. *J. R. Soc. Interface* 17, 20200569. <https://doi.org/10.1098/rsif.2020.0569>.
105. Ganske, A.S., and Uhl, G. (2018). The sensory equipment of a spider – a morphological survey of different types of sensillum in both sexes of *Argiope bruennichi* (Araneae, Araneidae). *Arthropod Struct. Dev.* 47, 144–161. <https://doi.org/10.1016/j.asd.2018.01.001>.
106. González-Santillán, E., and Prendini, L. (2013). Redefinition and generic revision of the north american vaejovid scorpion subfamily syntropinae kraepelin, 1905, with descriptions of six new genera. *Bull. Am. Mus. Nat. Hist.* 382, 1–71. <https://doi.org/10.1206/830.1>.
107. Lin, L.H., Edmonds, D.T., and Vollrath, F. (1995). Structural engineering of an orb spider's web. *Nature* 373, 146–148. <https://doi.org/10.1038/373146a0>.
108. Kawano, A., and Morassi, A. (2020). Can the spider hear the position of the prey? *Mech. Syst. Signal Process.* 143, 106838. <https://doi.org/10.1016/j.ymssp.2020.106838>.
109. Das, R., Kumar, A., Patel, A., Vijay, S., Saurabh, S., and Kumar, N. (2017). Biomechanical characterization of spider webs. *J. Mech. Behav. Biomed. Mater.* 67, 101–109. <https://doi.org/10.1016/j.jmbbm.2016.12.008>.
110. Masters, W.M. (1984). Vibrations in the orb webs of *Nuctenea sclopeteria* (Araneidae). *Behav. Ecol. Sociobiol.* 15, 217–223. <https://doi.org/10.1007/bf00292978>.
111. Landolfá, M.A., and Barth, F.G. (1996). Vibrations in the orb web of the spider *Nephila clavipes*: cues for discrimination and orientation. *J. Comp. Physiol.* 179. <https://doi.org/10.1007/BF00192316>.
112. Klärner, D., and Barth, F.G. (1982). Vibratory signals and prey capture in orb-weaving spiders (*Zygiella x-notata*, *Nephila clavipes*; Araneidae). *J. Comp. Physiol.* 148, 445–455. <https://doi.org/10.1007/BF00619783>.
113. Main, I.G. (1993). *Vibrations and Waves in Physics* (Cambridge University Press). <https://doi.org/10.1017/CBO9781139170567>.
114. Mortimer, B., Holland, C., Windmill, J.F.C., and Vollrath, F. (2015). Unpicking the signal thread of the sector web spider *Zygiella x-notata*. *J. R. Soc. Interface* 12, 20150633. <https://doi.org/10.1098/rsif.2015.0633>.
115. Mortimer, B., Soler, A., Siviour, C.R., Zaera, R., and Vollrath, F. (2016). Tuning the instrument: sonic properties in the spider's web. *J. R. Soc. Interface* 13, 20160341. <https://doi.org/10.1098/rsif.2016.0341>.
116. Wirth, E., and Barth, F. (1992). Forces in the spider orb web. *J. Comp. Physiol.* 171. <https://doi.org/10.1007/BF00223966>.
117. Watanabe, T. (2000). Web tuning of an orb web spider, *Octonoba sybotides*, regulated prey-catching behaviour. *Proc. Biol. Sci.* 267, 565–569. <https://doi.org/10.1098/rspb.2000.1038>.
118. Yang, T., Xu, S., and Kaewunruen, S. (2019). Nonlinear free vibrations of spider web structures. In *Proceedings of the 26th International Congress on Sound and Vibration (ICSV)*.
119. Kaewunruen, S., Ngamkhanong, C., and Xu, S. (2020). Large amplitude vibrations of imperfect spider web structures. *Sci. Rep.* 10, 19161. <https://doi.org/10.1038/s41598-02076269-x>.
120. Drodge, D.R., Mortimer, B., Holland, C., and Siviour, C.R. (2012). Ballistic impact to access the high-rate behaviour of individual silk fibres. *J. Mech. Phys. Solids* 60, 1710–1721. <https://doi.org/10.1016/j.jmps.2012.06.007>.

121. Boutry, C., and Blackledge, T.A. (2010). Evolution of supercontraction in spider silk: structure-function relationship from tarantulas to orb-weavers. *J. Exp. Biol.* 213, 3505–3514. <https://doi.org/10.1242/jeb.046110>.
122. Boutry, C., and Blackledge, T.A. (2013). Wetwebs work better: humidity, supercontraction and the performance of spider orb webs. *J. Exp. Biol.* 216, 3606–3610. <https://doi.org/10.1242/jeb.084236>.
123. Elices, M., Plaza, G.R., Pe' rez-Rigueiro, J., and Guinea, G.V. (2011). The hidden link between supercontraction and mechanical behavior of spider silks. *J. Mech. Behav. Biomed. Mater.* 4, 658–669. <https://doi.org/10.1016/j.jmbbm.2010.09.008>.
124. Liu, Y., Shao, Z., and Vollrath, F. (2005). Relationships between supercontraction and mechanical properties of spider silk. *Nat. Mater.* 4, 901–905. <https://doi.org/10.1038/nmat1534>.
125. Yazawa, K., Malay, A.D., Masunaga, H., Norma-Rashid, Y., and Numata, K. (2020). Simultaneous effect of strain rate and humidity on the structure and mechanical behavior of spider silk. *Commun. Mater.* 1, 10. <https://doi.org/10.1038/s43246-020-0011-8>.
126. Mortimer, B., Gordon, S.D., Holland, C., Siviour, C.R., Vollrath, F., and Windmill, J.F.C. (2014). The speed of sound in silk: linking material performance to biological function. *Adv. Mater.* 26, 5179–5183. <https://doi.org/10.1002/adma.201401027>.
127. Frohlich, C., and Buskirk, R.E. (1982). Transmission and attenuation of vibration in orb spider webs. *J. Theor. Biol.* 95, 13–36. [https://doi.org/10.1016/00225193\(82\)90284-3](https://doi.org/10.1016/00225193(82)90284-3).
128. Vollrath, F., and Selden, P. (2007). The role of behavior in the evolution of spiders, silks, and webs. *Annu. Rev. Ecol. Evol. Syst.* 38, 819–846. <https://doi.org/10.1146/annurev.ecolsys.37.091305.110221>.
129. Miniaci, M., Krushynska, A., Movchan, A.B., Bosia, F., and Pugno, N.M. (2016). Spider web-inspired acoustic metamaterials. *Appl. Phys. Lett.* 109, 071905. <https://doi.org/10.1063/1.4961307>.
130. Sepehri, S., Jafari, H., Mashhadi, M.M., Yazdi, M.R.H., and Fakhrabadi, M.M.S. (2020). Study of tunable locally resonant metamaterials: effects of spider-web and snowflake hierarchies. *Int. J. Solids Struct.* 204–205, 81–95. <https://doi.org/10.1016/j.ijsolstr.2020.08.014>.
131. Dal Poggetto, V.F., Bosia, F., Miniaci, M., and Pugno, N.M. (2021). Optimization of spider web-inspired phononic crystals to achieve tailored dispersion for diverse objectives. *Mater. Des.* 209, 109980. <https://doi.org/10.1016/j.matdes.2021.109980>.
132. Krushynska, A.O., Bosia, F., Miniaci, M., and Pugno, N.M. (2017). Spider web-structured labyrinthine acoustic metamaterials for low frequency sound control. *New J. Phys.* 19, 105001. <https://doi.org/10.1088/1367-2630/aa83f3>.
133. Huang, H., Cao, E., Zhao, M., Alamri, S., and Li, B. (2021). Spider web-inspired lightweight membrane-type acoustic metamaterials for broadband low-frequency sound isolation. *Polymers* 13, 1146. <https://doi.org/10.3390/polym13071146>.
134. Barth, F.G. (2004). Spider mechanoreceptors. *Curr. Opin. Neurobiol.* 14, 415–422. <https://doi.org/10.1016/j.conb.2004.07.005>.
135. Seo, J., Kim, K., Kim, H., and Moon, M. (2020). Lyriform vibration receptors in the webbuilding spider, *Nephila clavata* (Araneidae: Araneae: Arachnida). *Entomol. Res.* 50, 586–593. <https://doi.org/10.1111/1748-5967.12470>.
136. Barth, F.G. (2021). A spider in motion: facets of sensory guidance. *J. Comp. Physiol. A Neuroethol. Sens. Neural Behav. Physiol.* 207, 239–255. <https://doi.org/10.1007/s00359-02001449-z>.
137. Klopsch, C., Kuhlmann, H.C., and Barth, F.G. (2012). Airflow elicits a spider's jump towards airborne prey. I. Airflow around a flying blowfly. *J. R. Soc. Interface* 9, 2591–2602. <https://doi.org/10.1098/rsif.2012.0186>.
138. Klopsch, C., Kuhlmann, H.C., and Barth, F.G. (2013). Airflow elicits a spider's jump towards airborne prey. II. Flow characteristics guiding behaviour. *J. R. Soc. Interface* 10, 20120820. <https://doi.org/10.1098/rsif.2012.0820>.
139. Bathellier, B., Barth, F.G., Albert, J.T., and Humphrey, J.A.C. (2005). Viscosity-mediated motion coupling between pairs of trichobothria on the leg of the spider *Cupiennius salei*. *J. Comp. Physiol. A Neuroethol. Sens. Neural Behav. Physiol.* 191, 733–746. <https://doi.org/10.1007/s00359-0050629-5>.
140. Guarino, R., Greco, G., Mazzolai, B., and Pugno, N.M. (2019). Fluid-structure interaction study of spider's hair flow-sensing system. *Mater. Today Proc.* 7, 418–425. <https://doi.org/10.1016/j.matpr.2018.11.104>.
141. Young, S.L., Chyasnachyus, M., Erko, M., Barth, F.G., Fratzl, P., Zlotnikov, I., Politi, Y., and Tsukruk, V.V. (2014). A spider's biological vibration filter: micromechanical characteristics of a biomaterial surface. *Acta Biomater.* 10, 4832–4842. <https://doi.org/10.1016/j.actbio.2014.07.023>.
142. Erko, M., Younes-Metzler, O., Rack, A., Zaslansky, P., Young, S.L., Milliron, G., Chyasnachyus, M., Barth, F.G., Fratzl, P., Tsukruk, V., et al. (2015). Micro- and nanostructural details of a spider's filter for substrate vibrations: relevance for low frequency signal transmission. *J. R. Soc. Interface* 12, 20141111. <https://doi.org/10.1098/rsif.2014.1111>.
143. Dal Poggetto, V.F., Bosia, F., Greco, G., and Pugno, N.M. (2022). Prey impact localization enabled by material and structural interaction in spider orb webs. *Adv. Theory Simul.* 5, 2100282. <https://doi.org/10.1002/adts.202100282>.
144. Dijkstra, M., Baar, J.J.V., Wiegerink, R.J., Lammerink, T.S.J., Boer, J.H.D., and Krijnen, G.J.M. (2005). Artificial sensory hairs based on the flow sensitive receptor hairs of crickets. *J. Micromech. Microeng.* 15, S132–S138. <https://doi.org/10.1088/0960-1317/15/7/019>.
145. Wu, Z., Ai, J., Ma, Z., Zhang, X., Du, Z., Liu, Z., Chen, D., and Su, B. (2019). Flexible out-of-plane wind sensors with a self-powered feature inspired by fine hairs of the spider. *ACS Appl. Mater. Interfaces* 11, 44865–44873. <https://doi.org/10.1021/acsami.9b15382>.

146. Chen, N., Tucker, C., Engel, J.M., Yang, Y., Pandya, S., and Liu, C. (2007). Design and characterization of artificial haircell sensor for flow sensing with ultrahigh velocity and angular sensitivity. *J. Microelectromech. Syst.* 16, 999–1014. <https://doi.org/10.1109/JMEMS.2007.902436>.
147. Kang, D., Pikhitsa, P.V., Choi, Y.W., Lee, C., Shin, S.S., Piao, L., Park, B., Suh, K.Y., Kim, T.i., and Choi, M. (2014). Ultrasensitive mechanical crack-based sensor inspired by the spider sensory system. *Nature* 516, 222–226. <https://doi.org/10.1038/nature14002>.
148. Kim, T., Lee, T., Lee, G., Choi, Y., Kim, S., Kang, D., and Choi, M. (2018). Polyimide encapsulation of spider-inspired crack-based sensors for durability improvement. *Appl. Sci.* 8, 367. <https://doi.org/10.3390/app8030367>.
149. Zhou, J., and Miles, R.N. (2017). Sensing fluctuating airflow with spider silk. *Proc. Natl. Acad. Sci. USA* 114, 12120–12125. <https://doi.org/10.1073/pnas.1710559114>.
150. Stockmann, R. (2015). Introduction to scorpion biology and ecology. In *Scorpion Venoms*. [https://doi.org/10.1007/978-94-007-64040\\_14](https://doi.org/10.1007/978-94-007-64040_14).
151. O'Connell-Rodwell, C.E. (2007). Keeping an 'ear' to the ground: seismic communication in elephants. *Physiology* 22, 287–294. <https://doi.org/10.1152/physiol.00008.2007>.
152. Narins, P.M., Reichman, O.J., Jarvis, J.U., and Lewis, E.R. (1992). Seismic signal transmission between burrows of the Cape mole-rat, *Georchus capensis*. *J. Comp. Physiol.* 170, 13–21. <https://doi.org/10.1007/BF00190397>. 153. Brownell, P.H. (1977). Compressional and surface waves in sand: used by desert scorpions to locate prey. *Science* 197, 479–482. <https://doi.org/10.1126/science.197.4302.479>.
154. Brownell, P.H. (1984). Prey detection by the sand scorpion. *Sci. Am.* 251, 86–97. <https://doi.org/10.1038/scientificamerican1284-86>.
155. French, A.S., and Torkkeli, P.H. (2004). Mechanotransduction in spider slit sensilla. *Can. J. Physiol. Pharmacol.* 82, 541–548. <https://doi.org/10.1139/y04-031>.
156. Mineo, M.F., and Del Claro, K. (2006). Mechanoreceptive function of pectines in the Brazilian yellow scorpion *Tityus serrulatus*: perception of substrate-borne vibrations and prey detection. *Acta Ethol.* 9, 79–85. <https://doi.org/10.1007/s10211-006-0021-7>.
157. Brownell, P., and Farley, R.D. (1979). Orientation to vibrations in sand by the nocturnal scorpion *Paruroctonus mesaensis*: mechanism of target localization. *J. Comp. Physiol.* 131, 31–38. <https://doi.org/10.1007/BF00613081>.
158. Brownell, P., and Farley, R.D. (1979). Prey localizing behaviour of the nocturnal desert scorpion, *Paruroctonus mesaensis*: orientation to substrate vibrations. *Anim. Behav.* 27, 185–193. [https://doi.org/10.1016/0003-3472\(79\)90138-6](https://doi.org/10.1016/0003-3472(79)90138-6).
159. Brownell, P.H., and Leo van Hemmen, J. (2001). Vibration sensitivity and a computational theory for prey-localizing behavior in sand scorpions. *Am. Zool.* 41, 1229–1240. <https://doi.org/10.1093/icb/41.5.1229>.
160. Wang, K., Zhang, J., Liu, L., Chen, D., Song, H., Wang, Y., Niu, S., Han, Z., and Ren, L. (2019). Vibrational receptor of scorpion (*Heterometrus petersii*): the basitarsal compound slit sensilla. *J. Bionic Eng.* 16, 76–87. <https://doi.org/10.1007/s42235-0190008-5>.
161. Fratzl, P., Kolednik, O., Fischer, F.D., and Dean, M.N. (2016). The mechanics of tessellations-bioinspired strategies for fracture resistance. *Chem. Soc. Rev.* 45, 252–267. <https://doi.org/10.1039/c5cs00598a>.
162. Fratzl, P., and Barth, F.G. (2009). Biomaterial systems for mechanosensing and actuation. *Nature* 462, 442–448. <https://doi.org/10.1038/nature08603>.
163. Hill, P.S.M. (2009). How do animals use substrate-borne vibrations as an information source? *Naturwissenschaften* 96, 1355–1371. <https://doi.org/10.1007/s00114-009-0588-8>.
164. Mortimer, B., Rees, W.L., Koelemeijer, P., and Nissen-Meyer, T. (2018). Classifying elephant behaviour through seismic vibrations. *Curr. Biol.* 28, R547–R548. <https://doi.org/10.1016/j.cub.2018.03.062>.
165. Reinwald, M., Moseley, B., Szenicer, A., Nissen-Meyer, T., Oduor, S., Vollrath, F., Markham, A., and Mortimer, B. (2021). Seismic localization of elephant rumbles as a monitoring approach. *J. R. Soc. Interface* 18, 20210264. <https://doi.org/10.1098/rsif.2021.0264>.
166. Mortimer, B., Walker, J.A., Lolchuragi, D.S., Reinwald, M., and Daballen, D. (2021). Noise matters: elephants show risk avoidance behaviour in response to human-generated seismic cues. *Proc. Biol. Sci.* 288, 20210774. <https://doi.org/10.1098/rspb.2021.0774>.
167. Eaton, T.H., and Cott, H.B. (1940). Adaptive coloration in animals. *Am. Midl. Nat.* 24, 763. <https://doi.org/10.2307/2420875>.
168. Fenton, M.B. (2018). Predator-prey interactions: Co-evolution between bats and their prey. *Springer Briefs in Animal Sciences*. By David Steve Jacobs and Anna Bastian. Cham (Switzerland) and New York: Springer. \$54.99 (paper); \$39.99 (ebook). xi + 135 p.; ill.; index and index of species. ISBN: 978-3-319-32490-6 (pb); 978-3-31932492-0 (eb). 2016. *Q Rev Biol.* 93. <https://doi.org/10.1086/698066>.
169. Edmunds, M. (1974). *Defense in Animals: A Survey of Anti-predator Defenses* (Longman).
170. McClure, M., Clerc, C., Desbois, C., Meichanetzoglou, A., Cau, M., Bastin-Helene, L., Bacigalupo, J., Houssin, C., Pinna, C., Nay, B., et al. (2019). Why has transparency evolved in aposematic butterflies? Insights from the largest radiation of aposematic butterflies, the Ithomiini. *Proc. Biol. Sci.* 286, 20182769. <https://doi.org/10.1098/rspb.2018.2769>.
171. Rubin, J.J., Hamilton, C.A., McClure, C.J.W., Chadwell, B.A., Kawahara, A.Y., and Barber, J.R. (2018). The evolution of anti-bat sensory illusions in moths. *Sci. Adv.* 4, eaar7428. <https://doi.org/10.1126/sciadv.aar7428>.
172. Vamosi, S.M. (2005). On the role of enemies in divergence and diversification of prey: a review and synthesis. *Can. J. Zool.* 83, 894–910. <https://doi.org/10.1139/z05-063>.
173. Kelley, L.A., and Kelley, J.L. (2014). Animal visual illusion and confusion: the importance of a perceptual perspective. *Behav. Ecol.* 25, 450–463. <https://doi.org/10.1093/beheco/art118>.
174. Miller, L.A., and Surlykke, A. (2001). How some insects detect and avoid being eaten by bats: tactics and counter-tactics of prey and predator. *Bioscience* 51. [https://doi.org/10.1641/0006-3568\(2001\)051\[0570:HSIDAA\]2.0.CO;2](https://doi.org/10.1641/0006-3568(2001)051[0570:HSIDAA]2.0.CO;2).

175. Corcoran, A.J., and Hristov, N.I. (2014). Convergent evolution of anti-bat sounds. *J. Comp. Physiol. A Neuroethol. Sens. Neural Behav. Physiol.* 200, 811–821. <https://doi.org/10.1007/s00359-014-0924-0>.
176. Corcoran, A.J., Barber, J.R., and Conner, W.E. (2009). Tiger moth jams bat sonar. *Science* 325, 325–327. <https://doi.org/10.1126/science.1174096>.
177. Wohlgenuth, M.J., Luo, J., and Moss, C.F. (2016). Three-dimensional auditory localization in the echolocating bat. *Curr. Opin. Neurobiol.* 41, 78–86. <https://doi.org/10.1016/j.conb.2016.08.002>.
178. Shen, Z., Neil, T.R., Robert, D., Drinkwater, B.W., and Holderied, M.W. (2018). Biomechanics of a moth scale at ultrasonic frequencies. *Proc. Natl. Acad. Sci. USA* 115, 12200–12205. <https://doi.org/10.1073/pnas.1810025115>.
179. O'Reilly, L.J., Agassiz, D.J.L., Neil, T.R., and Holderied, M.W. (2019). Deaf moths employ acoustic Müllerian mimicry against bats using wingbeat-powered tymbals. *Sci. Rep.* 9, 1444. <https://doi.org/10.1038/s41598-018-37812-z>.
180. Zeng, J., Xiang, N., Jiang, L., Jones, G., Zheng, Y., Liu, B., and Zhang, S. (2011). Moth wing scales slightly increase the absorbance of bat echolocation calls. *PLoS One* 6, e27190. <https://doi.org/10.1371/journal.pone.0027190>.
181. Neil, T.R., Shen, Z., Robert, D., Drinkwater, B.W., and Holderied, M.W. (2020). Moth wings are acoustic metamaterials. *Proc. Natl. Acad. Sci. USA* 117, 31134–31141. <https://doi.org/10.1073/pnas.2014531117>.
182. Neil, T.R., Shen, Z., Robert, D., Drinkwater, B.W., and Holderied, M.W. (2020). Thoracic scales of moths as a stealth coating against bat biosonar. *J. R. Soc. Interface* 17, 20190692. <https://doi.org/10.1098/rsif.2019.0692>.
183. Barber, J.R., Leavell, B.C., Keener, A.L., Breinholt, J.W., Chadwell, B.A., McClure, C.J.W., Hill, G.M., and Kawahara, A.Y. (2015). Moth tails divert bat attack: evolution of acoustic deflection. *Proc. Natl. Acad. Sci. USA* 112, 2812–2816. <https://doi.org/10.1073/pnas.1421926112>.
184. Arenas, J.P., and Crocker, M.J. (2010). Recent trends in porous sound-absorbing materials. *Sound Vib.* 44.
185. Conner, W.E. (2014). Adaptive sounds and silences: acoustic anti-predator strategies in insects. In *Insect Hearing and Acoustic Communication. Animal Signals and Communication*, 1, B. Hedwig, ed. eds. [https://doi.org/10.1007/978-3-642-404627\\_5](https://doi.org/10.1007/978-3-642-404627_5).
186. Hegel, J.R., and Casey, T.M. (1982). Thermoregulation and control of head temperature in the sphinx moth, *manduca sexta*. *J. Exp. Biol.* 101, 1–15. <https://doi.org/10.1242/jeb.101.1.1>.
187. Lee, W.-J., and Moss, C.F. (2016). Can the elongated hindwing tails of fluttering moths serve as false sonar targets to divert bat attacks? *J. Acoust. Soc. Am.* 139, 2579. <https://doi.org/10.1121/1.4947423>.
188. Kirchner, W.H. (1993). Acoustical communication in honeybees. *Apidologie* 24, 297–307. <https://doi.org/10.1051/apido:19930309>.
189. Ono, M., Igarashi, T., Ohno, E., and Sasaki, M. (1995). Unusual thermal defence by a honeybee against mass attack by hornets. *Nature* 377, 334–336. <https://doi.org/10.1038/377334a0>.
190. Ugajin, A., Kiya, T., Kunieda, T., Ono, M., Yoshida, T., and Kubo, T. (2012). Detection of neural activity in the brains of Japanese honeybee workers during the formation of a "Hot defensive bee ball. *PLoS One* 7, e32902. <https://doi.org/10.1371/journal.pone.0032902>.
191. Schaber, C.F., Gorb, S.N., and Barth, F.G. (2012). Force transformation in spider strain sensors: white light interferometry. *J. R. Soc. Interface* 9, 1254–1264. <https://doi.org/10.1098/rsif.2011.0565>.
192. Greco, G., Mirbaha, H., Schmuck, B., Rising, A., and Pugno, N.M. (2022). Artificial and natural silk materials have high mechanical property variability regardless of sample size. *Sci. Rep.* 12, 3507. <https://doi.org/10.1038/s41598-022-07212-5>.
193. Klocke, D., and Schmitz, H. (2011). Water as a major modulator of the mechanical properties of insect cuticle. *Acta Biomater.* 7, 2935–2942. <https://doi.org/10.1016/j.actbio.2011.04.004>.
194. Work, R.W. (1977). Dimensions, birefringences, and force-elongation behavior of major and minor ampullate silk fibers from orb-web-spinning spiders—the effects of wetting on these properties. *Text. Res. J.* 47, 650–662. <https://doi.org/10.1177/004051757704701003>.
195. Polis, G.A. (1990). *The Biology of Scorpions* (Stanford University Press).
196. Droogendijk, H., De Boer, M.J., Sanders, R.G.P., and Krijnen, G.J.M. (2014). A biomimetic accelerometer inspired by the cricket's clavate hair. *J. R. Soc. Interface* 11, 20140438. <https://doi.org/10.1098/rsif.2014.0438>.
197. Fan, Z., Chen, J., Zou, J., Bullen, D., Liu, C., and Delcomyn, F. (2002). Design and fabrication of artificial lateral line flow sensors. *J. Micromech. Microeng.* 12, 322–661. <https://doi.org/10.1088/0960-1317/12/5/322>.
198. Au, W.W.L. (2004). Echolocation signals of wild dolphins. *Acoust Phys.* 50, 454–462. <https://doi.org/10.1134/1.1776224>.
199. Nihoul, J.C.J. (2004). Echolocation in bats and dolphins. *J. Mar. Syst.* 50, 283. <https://doi.org/10.1016/j.jmarsys.2004.01.009>.
200. Au, W.W.L. (1997). Echolocation in dolphins with a dolphin-bat comparison. *Bioacoustics* 8, 137–162. <https://doi.org/10.1080/09524622.1997.9753357>.
201. Melcón, M.L., Failla, M., and In'iguez, M.A. (2012). Echolocation behavior of franciscana dolphins (*Pontoporia blainvillei*) in the wild. *J. Acoust. Soc. Am.* 131, EL448–EL453. <https://doi.org/10.1121/1.4710837>.
202. Madsen, P.T., Lammers, M., Wisniewska, D., and Beedholm, K. (2013). Nasal sound production in echolocating delphinids (*Tursiops truncatus* and *Pseudorca crassidens*) is dynamic, but unilateral: clicking on the right side and whistling on the left side. *J. Exp. Biol.* 216, 4091–4102. <https://doi.org/10.1242/jeb.091306>.

203. Kloepper, L.N., Nachtigall, P.E., Donahue, M.J., and Breese, M. (2012). Active echolocation beam focusing in the false killer whale, *Pseudorca crassidens*. *J. Exp. Biol.* 215, 1306–1312. <https://doi.org/10.1242/jeb.066605>.
204. Hemila, S., Nummela, S., and Reuter, T. (2010). Anatomy and physics of the exceptional sensitivity of dolphin hearing (Odontoceti: cetacea). *J. Comp. Physiol. A Neuroethol. Sens. Neural Behav. Physiol.* 196, 165–179. <https://doi.org/10.1007/s00359-010-0504-x>.
205. Thewissen, J.G., and Hussain, S.T. (1993). Origin of underwater hearing in whales. *Nature* 361, 444–445. <https://doi.org/10.1038/361444a0>.
206. Cranford, T.W., Krysl, P., and Hildebrand, J.A. (2008). Acoustic pathways revealed: simulated sound transmission and reception in Cuvier's beaked whale (*Ziphius cavirostris*). *Bioinspir. Biomim.* 3, 016001. <https://doi.org/10.1088/1748-3182/3/1/016001>.
207. Wei, C., Hoffmann-Kuhnt, M., Au, W.W.L., Ho, A.Z.H., Matrai, E., Feng, W., Ketten, D.R., and Zhang, Y. (2021). Possible limitations of dolphin echolocation: a simulation study based on a cross-modal matching experiment. *Sci. Rep.* 11, 6689. <https://doi.org/10.1038/s41598-021-85063-2>.
208. Dible, S.A., Flint, J.A., and Lepper, P.A. (2009). On the role of periodic structures in the lower jaw of the atlantic bottlenose dolphin (*Tursiops truncatus*). *Bioinspir. Biomim.* 4, 015005. <https://doi.org/10.1088/1748-3182/4/1/015005>.
209. Norris, K.S., and Mohl, B. (1983). Canodontocetes debilitate prey with sound? *Am. Nat.* 122, 85–104. <https://doi.org/10.1086/284120>.
210. Benoit-Bird, K.J., Au, W.W.L., and Kastelein, R. (2006). Testing the odontocete acoustic prey debilitation hypothesis: No stunning results. *J. Acoust. Soc. Am.* 120, 1118–1123. <https://doi.org/10.1121/1.2211508>.
211. Au, W.W.L., and Benoit-Bird, K.J. (2003). Automatic gain control in the echolocation system of dolphins. *Nature* 423, 861–863. <https://doi.org/10.1038/nature01727>.
212. Nachtigall, P.E., and Supin, A.Y. (2008). A falsekiller whale adjusts its hearing when it echolocates. *J. Exp. Biol.* 211, 1714–1718. <https://doi.org/10.1242/jeb.013862>.
213. Parsons, E.C.M. (2017). Impacts of Navy sonar on whales and dolphins: now beyond a smoking gun? *Front. Mar. Sci.* 4. <https://doi.org/10.3389/fmars.2017.00295>.
214. Reinwald, M., Grimal, Q., Marchal, J., Catheline, S., and Boschi, L. (2018). Boneconducted sound in a dolphin's mandible: experimental investigation of elastic waves mediating information on sound source position. *J. Acoust. Soc. Am.* 144, 2213. <https://doi.org/10.1121/1.5063356>.
215. Cranford, T.W., Amundin, M., and Norris, K.S. (1996). Functional morphology and homology in the odontocete nasal complex: implications for sound generation. *J. Morphol.* 228. [https://doi.org/10.1002/\(SICI\)10974687\(199606\)228:3<223::AID-JMOR1>3.0.CO;2-3](https://doi.org/10.1002/(SICI)10974687(199606)228:3<223::AID-JMOR1>3.0.CO;2-3).
216. Jakobsen, L., Christensen-Dalsgaard, J., Juhl, P.M., and Elemans, C.P.H. (2021). How loud can you go? Physical and physiological constraints to producing high sound pressures in animal vocalizations. *Front. Ecol. Evol.* 9. <https://doi.org/10.3389/fevo.2021.657254>.
217. Rand, A.S., and Dudley, R. (1993). Frogs inhelium: the Anuran vocal sac is not a cavity resonator. *Physiol. Zool.* 66, 793–806. <https://doi.org/10.1086/physzool.66.5.30163824>.
218. Riede, T., Beckers, G.J.L., Blevins, W., and Suthers, R.A. (2004). Inflation of the esophagus and vocal tract filtering in ring doves. *J. Exp. Biol.* 207, 4025–4036. <https://doi.org/10.1242/jeb.01256>.
219. Riede, T., Tokuda, I.T., Munger, J.B., and Thomson, S.L. (2008). Mammalian laryngeal air sacs add variability to the vocal tract impedance: physical and computational modeling. *J. Acoust. Soc. Am.* 124, 634–647. <https://doi.org/10.1121/1.2924125>.
220. Dunn, J.C., Halenar, L.B., Davies, T.G., Cristobal-Azkarate, J., Reby, D., Sykes, D., Dengg, S., Fitch, W.T., and Knapp, L.A. (2015). Evolutionary trade-off between vocal tract and testes dimensions in howler monkeys. *Curr. Biol.* 25, 2839–2844. <https://doi.org/10.1016/j.cub.2015.09.029>.
221. Veselka, N., McErlain, D.D., Holdsworth, D.W., Eger, J.L., Chhem, R.K., Mason, M.J., Brain, K.L., Faure, P.A., and Fenton, M.B. (2010). A bony connection signals laryngeal echolocation in bats. *Nature* 463, 939–942. <https://doi.org/10.1038/nature08737>.
222. Mhatre, N., Malkin, R., Deb, R., Balakrishnan, R., and Robert, D. (2017). Tree crickets optimize the acoustics of baffles to exaggerate their mate-attraction signal. *Elife* 6, e32763. <https://doi.org/10.7554/eLife.32763>.
223. Byrne, R.W., and da Cunha, R.G.T. (2006). Roars of black howler monkeys (*Alouatta caraya*): evidence for a function in inter-group spacing. *Behaviour* 143, 1169–1199. <https://doi.org/10.1163/156853906778691568>.
224. Schoen Ybarra, M. (1988). Morphological adaptations for loud phonation in the vocal organ of howling monkeys. *Primate Rep* 22.
225. Fitch, W.T., and Hauser, M.D. (1995). Vocal production in nonhuman primates: acoustics, physiology, and functional constraints on “honest” advertisement. *Am. J. Primatol.* 37, 191–219. <https://doi.org/10.1002/ajp.1350370303>.
226. Haimoff, E.H. (1983). Brief report: occurrence of anti-resonance in the song of the siamang (*Hylobates syndactylus*). *Am. J. Primatol.* 5, 249–256. <https://doi.org/10.1002/ajp.1350050309>.
227. Robles, L., and Ruggero, M.A. (2001). Mechanics of the mammalian cochlea. *Physiol. Rev.* 81, 1305–1352. <https://doi.org/10.1152/physrev.2001.81.3.1305>.
228. Reichenbach, T., and Hudspeth, A.J. (2014). The physics of hearing: fluid mechanics and the active process of the inner ear. *Rep. Prog. Phys.* 77, 076601. <https://doi.org/10.1088/0034-4885/77/7/076601>.
229. von Bekésy, G., and Peake, W.T. (1990). Experiments in hearing. *J. Acoust. Soc. Am.* 88, 2905. <https://doi.org/10.1121/1.399656>.
230. Emadi, G., Richter, C.P., and Dallos, P. (2004). Stiffness of the gerbil basilar membrane: radial and longitudinal variations. *J. Neurophysiol.* 91, 474–488. <https://doi.org/>



10.1152/jn.00446.2003.

231. LR, W. (1898). The theory of sound. *Nature* 58, 121–122. <https://doi.org/10.1038/058121a0>.
232. Rupin, M., Lerosey, G., De Rosny, J., and Lemoult, F. (2019). Mimicking the cochlea with an active acoustic metamaterial. *New J. Phys.* 21, 093012. <https://doi.org/10.1088/13672630/ab3d8f>.
233. Fettiplace, R., and Nam, J.H. (2019). Tonotopyin calcium homeostasis and vulnerability of cochlear hair cells. *Hear. Res.* 376, 11–21. <https://doi.org/10.1016/j.heares.2018.11.002>.
234. Ma, F., Wu, J.H., Huang, M., Fu, G., and Bai, C. (2014). Cochlear bionic acoustic metamaterials. *Appl. Phys. Lett.* 105, 213702. <https://doi.org/10.1063/1.4902869>.
235. Egui'luz, V.M., Ospeck, M., Choe, Y., Hudspeth, A.J., and Magnasco, M.O. (2000). Essential nonlinearities in hearing. *Phys. Rev. Lett.* 84, 5232–5235. <https://doi.org/10.1103/PhysRevLett.84.5232>.
236. Hudspeth, A.J., Ju'licher, F., and Martin, P. (2010). A critique of the critical cochlea: hopf A bifurcation - is better than none. *J. Neurophysiol.* 104, 1219–1229. <https://doi.org/10.1152/jn.00437.2010>.
237. Kemp, D.T. (1979). Evidence of mechanicalnonlinearity and frequency selective wave amplification in the cochlea. *Arch. Oto-Rhino-Laryngol.* 224, 37–45. <https://doi.org/10.1007/BF00455222>.
238. Ruggero, M.A., Rich, N.C., and Recio, A. (1996). The effect of intense acoustic stimulation on basilar-membrane vibrations. *Audit Neurosci.* 2, 216.
239. Ren, T., He, W., and Gillespie, P.G. (2011). Measurement of cochlear power gain in the sensitive gerbil ear. *Nat. Commun.* 2, 216. <https://doi.org/10.1038/ncomms1226>.
240. De Boer, E. (1996). Mechanics of the cochlea: modeling efforts. In *The Cochlea*, Springer Handbook of Auditory Research, 8, P. Dallos, A.N. Popper, and R.R. Fay, eds (Springer). [https://doi.org/10.1007/978-1-4612-07573\\_5](https://doi.org/10.1007/978-1-4612-07573_5).
241. Ni, G., Elliott, S.J., Ayat, M., and Teal, P.D. (2014). Modelling cochlear mechanics. *BioMed Res. Int.* 2014, 150637. <https://doi.org/10.1155/2014/150637>.
242. Manoussaki, D., Dimitriadis, E.K., and Chadwick, R.S. (2006). Cochlea's graded curvature effect on low frequency waves. *Phys. Rev. Lett.* 96, 088701. <https://doi.org/10.1103/PhysRevLett.96.088701>.
243. Manoussaki, D., Chadwick, R.S., Ketten, D.R., Arruda, J., Dimitriadis, E.K., and O'Malley, J.T. (2008). The influence of cochlear shape on low-frequency hearing. *Proc. Natl. Acad. Sci. USA* 105, 6162–6166. <https://doi.org/10.1073/pnas.0710037105>.
244. Zhao, L., and Zhou, S. (2019). Compactacoustic rainbow trapping in a bioinspired spiral array of graded locally resonant metamaterials. *Sensors* 19, E788. <https://doi.org/10.3390/s19040788>.
245. Karlos, A., and Elliott, S.J. (2020). Cochleainspired design of an acoustic rainbow sensor with a smoothly varying frequency response. *Sci. Rep.* 10, 10803. <https://doi.org/10.1038/s41598-020-67608-z>.
246. Gu, G.X., Dimas, L., Qin, Z., and Buehler, M.J. (2016). Optimization of composite fracture properties: method, validation, and applications. *J. Appl. Mech.* 83. <https://doi.org/10.1115/1.4033381>.
247. Diaz, A.R., Haddow, A.G., and Ma, L. (2005). Design of band-gap grid structures. *Struct. Multidiscipl. Optim.* 29, 418–431. <https://doi.org/10.1007/s00158-004-0497-6>.
248. Halkjær, S., Sigmund, O., and Jensen, J.S. (2005). Inverse design of phononic crystals by topology optimization. *Z. für Kristallogr. Cryst. Mater.* 220, 895–905. <https://doi.org/10.1524/zkri.2005.220.9-10.895>.
249. Hedayatrasa, S., Abhary, K., and Uddin, M. (2015). Numerical study and topology optimization of 1D periodic bimaterial phononic crystal plates for bandgaps of low order Lamb waves. *Ultrasonics* 57, 104–124. <https://doi.org/10.1016/j.ultras.2014.11.001>.
250. Chen, Y., Huang, X., Sun, G., Yan, X., and Li, G. (2017). Maximizing spatial decay of evanescent waves in phononic crystals by topology optimization. *Comput. Struct.* 182, 430–447. <https://doi.org/10.1016/j.compstruc.2017.01.001>.
251. Wilm, M., Ballandras, S., Laude, V., and Pastureaud, T. (2002). A full 3D plane-wave expansion model for 1-3 piezoelectric composite structures. *J. Acoust. Soc. Am.* 112, 943–952. <https://doi.org/10.1121/1.1496081>.
252. Mace, B.R., and Manconi, E. (2008). Modelling wave propagation in two-dimensional structures using finite element analysis. *J. Sound Vib.* 318, 884–902. <https://doi.org/10.1016/j.jsv.2008.04.039>.
253. Kafesaki, M., and Economou, E.N. (1999). Multiple-scattering theory for three-dimensional periodic acoustic composites. *Phys. Rev. B* 60, 11993–12001. <https://doi.org/10.1103/PhysRevB.60.11993>.
254. Xie, L., Xia, B., Liu, J., Huang, G., and Lei, J. (2017). An improved fast plane wave expansion method for topology optimization of phononic crystals. *Int. J. Mech. Sci.* 120, 171–181. <https://doi.org/10.1016/j.ijmecsci.2016.11.023>.
255. D'Alessandro, L., Bahr, B., Daniel, L., Weinstein, D., and Ardito, R. (2017). Shape optimization of solid-air porous phononic crystal slabs with widest full 3D bandgap for in-plane acoustic waves. *J. Comput. Phys.* 344, 465–484. <https://doi.org/10.1016/j.jcp.2017.05.018>.
256. Costagliola, G., Guarino, R., Borgia, F., Gkagkas, K., and Pugno, N.M. (2020). Evolutionary algorithm optimization of staggered biological or biomimetic composites using the random fuse model. *Phys. Rev. Appl.* 13, 034049. <https://doi.org/10.1103/PhysRevApplied.13.034049>.
257. Han, X.K., and Zhang, Z. (2019). Topological optimization of phononic crystal thin plate by a genetic algorithm. *Sci. Rep.* 9, 8331. <https://doi.org/10.1038/s41598-019-44850-8>.

258. Liu, R., Kumar, A., Chen, Z., Agrawal, A., Sundararaghavan, V., and Choudhary, A. (2015). A predictive machine learning approach for microstructure optimization and materials design. *Sci. Rep.* 5, 11551. <https://doi.org/10.1038/srep11551>.
259. Jin, Y., He, L., Wen, Z., Mortazavi, B., Guo, H., Torrent, D., Djafari-Rouhani, B., Rabczuk, T., Zhuang, X., and Li, Y. (2022). Intelligent ondemand design of phononic metamaterials. *Nanophotonics* 11, 439–460. <https://doi.org/10.1515/nanoph-2021-0639>.
260. Chatterjee, T., Chakraborty, S., Goswami, S., Adhikari, S., and Friswell, M.I. (2021). Robust topological designs for extreme metamaterial micro-structures. *Sci. Rep.* 11, 15221. <https://doi.org/10.1038/s41598-02194520-x>.
261. Zhang, H., Luo, Y., and Kang, Z. (2018). Bimaterial microstructural design of chiral auxetic metamaterials using topology optimization. *Compos. Struct.* 195, 232–248. <https://doi.org/10.1016/j.compstruct.2018.04.058>.